LARS Technical Report 082181

A Study of the Spectral Reflectance of Selected Eroded Soils of Indiana in Relationship to Their Chemical and Physical Properties

Kathleen Latz
Richard A. Weismiller
George E. Van Scoyoc

Laboratory for Applications of Remote Sensing
Purdue University West Lafayette, Indiana 47906 USA
1981

LARS Technical Report 082181

A STUDY OF THE SPECTRAL REFLECTANCE OF SELECTED ERODED SOILS OF INDIANA IN RELATIONSHIP TO THEIR CHEMICAL AND PHYSICAL PROPERTIES

Kathleen Latz

Richard A. Weismiller

George E. Van Scoyoc

Purdue University
Laboratory for Applications of Remote Sensing
West Lafayette, Indiana 47906-1399, U.S.A.

August 1981

TABLE OF CONTENTS

LIST OF TABLES

LIST OF FIGURES

ABSTRACT

The loss of agriculturally productive soil by water erosion is a serious problem. In order to develop agricultural practices to decrease this loss of fertile cropland and prevent stream pollution from water run-off, a method of identifying, mapping and monitoring soil erosion is needed.

A study of eroded soils collected from different locations in Indiana was conducted to investigate the relationship between the chemical and physical properties and the spectral reflectance of these soils. Soil samples included six eroded toposequences (topographic sequences) with varying degrees of erosion and representing the three primary soil orders common in Indiana, i.e., Mollisol, Alfisol and Ultisol. Another series of soil samples was collected by depth from an Alfisol profile. These samples were used to compare an assimilated erosional condition to the naturally eroded toposequences.

All soil samples were prepared and analyzed under similar laboratory conditions. Analysis included organic carbon, total and amorphous iron oxide, particle size, moisture content and continuous scan spectral reflectance measurements. Three curve types were identifiable from the spectral reflectance. The Type 1 curve was indicative of the higher organic matter, uneroded soils of the Mollisols. The Type 2 curve was characteristic of soils having a lower organic matter content and better drainage than soils characterized by the Type 1 curve. The Type 2 curve was descriptive of the eroded Mollisol and uneroded Alfisol and Ultisol spectral curves. The Type 3 curve represented the eroded Alfisols and Ultisols, in addition to the uneroded Ultisols with higher iron oxide content.

The most important chemical properties affecting the spectral reflectance of these soils appeared to be the organic matter and iron oxide contents. It was observed that lower amounts of organic matter may have allowed the iron oxide to strongly influence the shape of the spectral curves of the eroded soils. Evidence of the eroded soils was most clearly seen around the 0.8 μm wavelength of the spectrum (bands 3 to 4 in the simulated Landsat graphs) by a distinct leveling off of the spectral curve. This decrease in slope was often prevalent where the degree of erosion was more severe.

A definite relationship between the laboratory spectral reflectance scan and the simulated Landsat graphs was apparent, suggesting that satellite data of eroded soil could provide useful information for the identification and detection of eroded soils.

INTRODUCTION

Degradation of soil by water erosion has been a problem for thousands of years. However, within the past four decades organizations such as the Soil Conservation Service (SCS), Environmental Protection Agency (EPA), Bureau of Reclamation, and Food and Agriculture Organization of the United Nations (FAO), have been taking an active role in soil conservation. Their interests lie in identifying active and potential areas of soil loss, measuring surface run-off to monitor sediment build-up and pesticide contamination of streams and waterways, and monitoring strip mining operations to prevent the loss of barren overburden.

In order to maintain the capability for food and fiber production, agriculture's most fertile soil must be preserved through soil conservation practices. Contour farming on steep slopes, planting grass in surface drainage ditches, or growing a cover crop to stabilize barren soil are several soil conservation practices used today. In order to be able to apply conservation practices to the soil, methods of detecting and monitoring soil erosion are essential. As of yet, no inexpensive method of effectively detecting soil erosion has been discovered. For soil surveyors to walk large areas of land to locate and map areas of erosion is time-consuming and inefficient. It would be very difficult and strenuous, if not impossible, for someone to walk unexplored land in Africa or even the U.S. and locate problem regions, large or small, with any degree of accuracy.

Early in the 1920's, soil surveyors recognized that the view of the landscape as seen from an airplane offered them a different perspective of the soil. Topographic differences in the landscape could be seen by the light and dark tonal variations of the soil. These tonal changes were also indicative of different drainage classes and erosional phases in the soil sequence. Within several years, soil surveyors incorporated the use of black-and-white aerial photographs as base maps. Today, black-and-white film is still a valuable tool used by the soil surveyor. As the efficiency and accuracy of mapping soils increased, so did the interest in developing additional methods of analyzing aerial photographs. The development of color film ranging from 0.4 to 0.7 μm in the visible portion of the electromagnetic spectrum led to further discoveries, including the ability to photograph in the near infrared region of the spectrum from 0.7 to 0.9 μm, a region not accessible to the human eye.

Man's needs for better and more efficient methods of identifying soils and their parameters continued to grow, as did the development of remote sensing instruments and techniques to assist him. In the 1960's, the advent

of the multispectral scanner made it possible to measure the spectral reflectance of soils, quantifying the percent of reflective light. Laboratory studies correlated chemical and physical data with the spectral reflectance, making inferences on soil parameters such as organic matter content, moisture content, and color. As it became necessary to make correlations between the laboratory data and field data, the multispectral scanner was moved from higher and higher platforms, to airplanes, and in 1972, onto an earth-orbiting satellite. The whole earth could now be seen from space. By using the sun's radiance as the source of energy, the spectral reflectance from objects on the earth could be measured by the satellite-borne instruments. These data are transmitted to earth where trained scientists analyze it.

This study describes the investigation of the relationship between a laboratory study of the chemical and physical properties of eroded soils to their spectral reflectance. The soil parameters studied include organic carbon content, particle size, iron oxide content, color, and spectral reflectance. All reflectance measurements were made at a uniform moisture tension to avoid differences in reflectance due to varying water tension in the soils.

By establishing these relationships using laboratory data, investigations can be extended to spectral reflectance collected by satellite instruments. This information will allow future identification, inventory, and monitoring of the erosional status of soils. Through this, erosion control practices can be implemented and reduce the loss of productive agricultural land.

LITERATURE REVIEW

History of Soil Erosion

Soil degradation and its effects have been studied as early as 7000 years ago (Lowdermilk, 1953), but only within this century have organizations been established with the objectives of identifying, mapping, and monitoring soil losses in order to implement erosion control practices. Approximately 40 years ago, the first organization devoted specifically to the control of soil erosion, the Soil Erosion Service, was formed by the United States Department of the Interior. Upon the urging of H. H. Bennett, the Soil Conservation Service (SCS), was established in 1935 as a permanent bureau of the United States Department of Agriculture (USDA) (Kohnke and Bertrand, 1959). Since that time, other federal agencies including the Environmental Protection Agency (EPA), the Bureau of Reclamation, and the Science and Education Administration (SEA), formerly the Agricultural Research Service (ARS), have concentrated efforts upon soil erosion studies and control.

Between the early 1930's and mid-1950's the USDA in cooperation with land grant colleges established erosion research stations at 48 locations in 26 states. Researchers studied and quantified the effects of topography,

cropping systems, management techniques, and potential erosion control practices using experimental field plots, and supplementing these with laboratory research (Soil Erosion: Prediction and Control, 1976). The data from these studies provided invaluable information about basic erosion principles, including measurements on run-off and soil losses. Other researchers have concentrated on methods of reducing the loss of fertile cropland and subsequent stream pollution, and reclaiming barren strip-mine overburden.

Despite this research, estimations of soil losses due to erosion, including wind and water, are devastatingly high. In 1959, Kohnke and Bertrand concluded that 50 million acres of cropland were severely eroded, and another 100 million acres of cropland were on the verge of being lost to erosion. An estimation of 500,000 acres annually is rendered unfit for practical cultivation, due to the shallow depth of the solum, the A and B horizons which support plant growth. Kimberlin (1976) estimated that two-thirds of the nation's cropland is losing soil at rates up to 5 tons per acre, while nearly 15% is losing more than 10 tons per acre per year. Other staggering estimates report that at present rates over one-half ton of soil per year for every man, woman, and child on the planet will be lost by erosion (United Nations Environment Program, 1977).

The FAO (1979) realized that only when the seriousness of the land degradation problem is recognized, and its causes properly identified, will it be possible to develop agricultural practices and to design and apply conservation measures that will ensure proper use of the land. In a report on "Methodology for Assessing Soil Degradation," FAO (1978) stated that due to the scarcity of reliable data, it was recommended that laboratory and field data on erosion be integrated with other methods of analysis, i.e., remote sensing, in an attempt to provide more precise information and stimulate countries to take actions to alleviate soil degradation.

History of Remote Sensing

Early advances in remote sensing were achieved by moving cameras from higher and higher platforms (Fink, 1980), to captive balloons, and into airplanes. As early as 1918, soil surveyors recognized that valuable information about the landscape could be gained from aerial observations (Bushnell, 1951). In the early 1920's, black-and-white aerial photographs replaced the base maps used by soil surveyors, and are still being used today.

Further experimentation in photographic film led to the development of color and near infrared film in the visible and infrared portions of the electromagnetic spectrum, 0.4 to 0.7 μm and 0.7 to 0.9 μm, respectively. Near infrared film has the advantage that it allows man to see past the range of the eye into the infrared region of the spectrum.

As man's need for more efficient methods of identifying soils and their parameters expanded, so the development of remote sensing instruments and

techniques grew (Manual of Remote Sensing, 1975). In the 1960's, the advent of instruments such as the spectrophotometer, multispectral scanner (MSS), and spectroradiometer along with computer-assisted pattern recognition techniques for sorting and classifying quantitative multispectral data made it possible to extend the study of the spectral properties of soil beyond the visible portion of the spectrum (Carroll, 1973b; Weismiller and Kaminsky, 1978).

Obukhov and Orlov (1964) found that the radiant energy of the sun is partially absorbed by the soil surface, which is chiefly transformed into heat. A small part of this energy is diffusely reflected, and this reflection is associated with a very important diagnostic property of soils - their color. This diffuse reflection may also play a part in objective estimation of the soil color, development of rapid quantitative methods of soil analysis, and aerial photo survey of soils.

A laboratory study conducted by Condit (1970), using a spectrophotometer, measured the spectral reflectance of 160 soil samples collected from 36 states. Measurements were made of both wet and dry samples, from 0.32 to 1.00 μm. The samples represented a wide variation in both color and reflectance. After examination of the 160 sets of curves, it was concluded that these soils could be classified into three general types with respect to their curve shape, and that as few as five wavelengths would be sufficient to predict reflection data. The wavelengths were 0.44, 0.54, 0.64, 0.74, and 0.86 μm.

Stoner and Baumgardner (1980) supported Condit's study, but identified two additional curves due to a broader spectral range from 0.52 to 2.32 μm. As described by Stoner and Baumgardner,

> "Type 1 curves exhibit rather low reflectance with a slightly increasing slope which gives them their characteristic concave form from 0.32 to about 1.0 μm. However, from about 1.0 to 1.3 μm the slope is seen to be nearly constant for these soils.
>
> "Type 2 curves are characterized by a generally decreasing slope to about 0.6 μm, followed by a slight dip from 0.6 to 0.7 μm, with continued decreasing slope beyond 0.75 μm. The result is a typical convex shaped curve from the visible to 1.3 μm. It has been observed that Type 2 soils tend to be better drained and lower in organic matter content than Type 1 soils.
>
> "The third type of soil reflectance curve observed by Condit shows a slightly decreasing steep slope to about 0.6 μm, followed by a slight dip from 0.62 to 0.74 μm with the slope decreasing to near zero or even becoming negative from 0.76 to 0.88 μm. Beyond 0.88 μm (to 1.0 μm) the slope increases with increasing wavelength. Moderately high free iron contents are observed in most Type 3 soils.

"Although similar in some respects to the Type 3 curve, a fourth curve type is seen to exhibit decreasing slope from 0.88 to 1.0 μm with the slope decreasing to zero and becoming negative from 1.0 to 1.3 μm. This fourth curve type has been observed in soils high in iron content and also high in organic matter.

"Yet another modification of the Type 3 curve shape which could be considered a fifth characteristic curve type is that in which the slope drops to zero and becomes negative from 0.75 μm to 1.3 μm. In this curve type, the reflectance at 1.3 μm is actually lower than the reflectance in the red portion of the spectrum. Only this fifth curve has been observed not to show the strong water absorption band at 1.45 μm, while every soil in this study shows the strong water absorption band at 1.95 μm. Soils showing this fifth curve type are very high in iron content with low organic matter contents.

Preliminary studies of soils using airborne multispectral data differentiated six soil surface conditions, from dark to light soils, including intermediate tones, each mapped with reasonable accuracy by computer techniques (Kristof, 1971). Another study used multispectral data to produce maps showing the location of five levels of organic matter content in soils (Baumgardner et al., 1970).

In 1972, a four-band multispectral scanner was mounted on the Landsat satellite (ERTS-1), providing complete images of large areas of the earth's surface, with 1.1 acre (.45 ha) spacial resolution elements within a 12,700 square mile (33,000 sq. km) image frame. The four bands range from 0.5 to 1.1 μm, including two bands in the visible region (0.5 to 0.6 μm and 0.6 to 0.7 μm) and two bands in the near infrared region (0.7 to 0.8 μm and 0.8 to 1.1 μm). These data are processed to provide imagery in the form of various photographic products as well as numerical format magnetic tapes for digital analysis (Stoner and Baumgardner, 1980). Satellite imagery allows the opportunity for repetitive, annual or seasonal, multispectral examination and monitoring of the earth in 18-day cycles. It can provide data over areas where the quality of information is poor or where no other sources are available (FAO, 1979).

Westin and Frazee (1976) recognized that Landsat imagery provided certain unique characteristics that aided in delineating soil association boundaries. Several of these characteristics were the synoptic view of 8.4 million acres (3.5 million ha) on which the condition of the soils and stage of vegetative growth were recorded at the same moment; the near-orthographic characteristic of the scenes, allowing for the construction of mosaics; and the temporal feature, permitting the study of soils and vegetation with time.

In a study of Clinton County, Indiana, using digital analysis of Landsat MSS data, results indicated that internal soil drainage characteristics could be identified. By correlating the drainage characteristics with the soil series, soil mapping units could be more accurately defined (Kirschner et

al., 1978). The success in preparing soil association maps and methods of using ancillary data, such as physiographic boundaries, prompted the initial preparation of a parent material map that could be coupled with Landsat MSS data to produce a spectral soil map with designated soil series (Weismiller and Kaminsky, 1978). A spectral classification of Jasper County, Indiana, printed in field sheet size printouts (scale of 1:15,840) accompanied the aerial photo in the soil mapping investigation. Delineation of soil drainage within parent material areas indicated the probable soils series present (Kaminsky et al., 1979).

Remote sensing, used as an additional tool in soil survey, can improve the accuracy and efficiency of soil mapping by providing "a priori" knowledge of the soils and their boundaries, and information where little or no other sources are available. To comprehend this mass of data made available by Landsat multispectral imagery, scientists must also be able to understand the relationship between chemical and physical characteristics of soils and soil reflectance properties.

In addition to delineating soil differences for use as an aid in soil mapping, closer observations of the spectral data have indicated the potential for separating erosion classes (Baumgardner et al., 1970; Matthews et al., 1973a; Kirschner, 1979; and Guruswamy et al., 1980). In a study conducted by FAO (1978), Landsat imagery was adequately demonstrated as a necessary first-stage input into the Soil Degradation Map of the World (scale of 1:5,000,000). Satellite-derived observations provided important data about slope lengths, vegetation covers, land use types, areas of predominant water, wind, or salinity degradation and inferences as to the rates at which these occurred.

Seubert et al. (1979) supported previous results showing that digital analysis of Landsat multispectral data could be used to detect and delineate severely eroded bare soil areas. In the study area of Whitley County, Indiana, nine spectral classes were clearly separable. These spectral classes corresponded to vegetation, water, classes of soil/vegetation complexes, and five classes of bare soil. The vegetation was identified as predominantly deciduous forest, while the mixed classes were row crops where the canopy had not completely covered the soil. The five bare soil classes formed a continuum from low to high spectral reflectance, where the low reflecting class represented the poorly drained soils in the landscape and the highest reflecting class correlated with the severely eroded upland soil.

To aid in determining the relationship between reflectance data collected by satellite and properties of eroded soils, a laboratory investigation was conducted. A continuous radiometric scan from 0.52 to 2.32 μm was taken of four soils in a Martinsville topographic sequence from Whitley County, Indiana. The soil occupying the lowest position in the sequence (DEPOSIT) had a dark surface color and represented the accumulation of soils eroded from higher positions in the landscape. The next soil up the sequence (MODERATE) was at the toe slope, which had a moderate degree of erosion. The third soil in the sequence (SEVERE) occupied the steepest portion of the slope, and was severely eroded. The uppermost soil in the sequence (SURFACE) had little slope and was slightly or non-eroded.

With the exception of the water absorption bands at 1.45 and 1.92 μm, the spectral curves showed that as the degree of soil erosion increased, the soil reflectance increased. Graphically illustrated, the severely eroded soil had the highest reflectance, and the moderately eroded soil displayed the second highest. The surface soil was the third lightest and the depositional soil had the lowest reflectance. The region of best separability of the reflectance curves was in the 0.5 to 1.1 μm range. At wavelengths greater than 1.1 μm, the severe and moderate erosion curves were unseparable.

Surface soil samples were also taken from two severely eroded Morley soils in Whitley County, Indiana, and spectral scans were taken. These two soils appeared similar in reflectance to the severely eroded soil in the Martinsville sequence. The curves of these soils showed a slightly decreasing, convex-shaped slope to about 0.6 μm, followed by a slight dip from about 0.6 to 0.75 μm with the slope decreasing to near zero from 0.75 to 0.9 μm. Beyond 0.9 to 1.0 μm, the slope increased with increasing wavelength. Seubert et al. (1979) suggested that even though soils may have differences in parent material or be separated geographically, certain properties characteristic to soil erosion may give similar responses. Although the nature of these properties was not investigated in detail in this study, previous and on-going work at the Laboratory for Applications of Remote Sensing (LARS) indicated that organic matter, clay mineralogy, soil texture, iron oxide and soil moisture content are important factors to be considered in soil reflectance (Al-Abbas et al., 1972; Beck et al., 1976; Montgomery et al., 1976; and Stoner and Baumgardner, 1980). It is likely that one or a combination of these factors is responsible for the distinct spectral patterns of eroded soils.

Soil Parameters

Particle Size

In a study of the relationship between particle sizes of soil aggregates and reflectance, Obukhov and Orlov (1964) found that the change in reflectivity is associated only with the diameter and shape of the aggregates and not with their chemical or mineralogical composition. They observed that fractions less than 0.25 mm in diameter have maximum reflectivity, while fractions 5 to 10 mm in diameter have the minimum. Further investigations by Orlov (1966) explained how the artificial breakdown of aggregates caused an increase in reflectance. It was observed that the fine particles fill the volume more completely, thus providing a more even surface. Coarse aggregates, having irregular shapes, form a very complex surface with a large number of pore spaces. As light falls on large, irregular shaped aggregates, most of the light flux penetrates into light traps and is completely extinguished there. Orlov found that particles less than 0.25 mm in diameter increased reflectance, indicating that this may be due to the residual products of weathering (particularly silica) that have their own high reflection coefficients. Bowers and Hanks (1965) found similar results by

measuring the reflectance of various-size fractions of bentonite and kaolinite clay minerals that had been oven-dried and sieved. The reflectance, measured by a spectrophotometer from 0.185 to 3.5 μm, for kaolinite was much greater than for bentonite, but both showed a rapid exponential increase with decreasing particle size.

Stoner and Baumgardner (1980) observed that decreasing the particle size among sand-textured soils increased soil reflectance, while the inverse was true for medium to fine textured soils. Slight reflectance differences could be seen in the 2.08 to 2.32 μm middle infrared region, where the reflectance decreased with finer and finer textures. In this case, reflectance differences could not be explained in terms of individual particles filling voids, but rather this correlation may be due to the associated increase in moisture content with increasing clay content in the soils.

Variations in soil reflectance can also be affected by the relative proportion of sand, silt, and clay in the soil. Al-Abbas et al. (1972) stated that decreasing the clay content of soils increased the spectral response, but found no clearly defined relationship between clay content and relative reflectance, hypothesizing that the relationship may be secondary due to the high correlation between organic matter and clay content. Matthews et al. (1973b) noticed that the reflectance of the Ap horizon was distinctly different from that of the B horizon in a Hagerstown silt loam profile. The reflectance curve of the Ap horizon exhibited broad, weak absorption bands at 1.4 and 2.2 μm, while the subsoil horizons had similar reflectance properties with stronger absorption bands at 0.9, 1.4, 1.9 and 2.2 μm. The absorption band at 0.9 μm was associated with high iron oxide content of this soil. Montgomery et al. (1976) observed that clay content was significant around the absorption bands at 1.4, 1.9 and 2.2 μm, and in the 0.5 to 0.7 μm range of the spectrum. The absorption bands are associated with increases in moisture content; as the amount of clay in soil increases, so does the influence from adsorbed water. Beck et al. (1976), relating spectral characteristics to specific soil properties, stated that the best range for determining clay content was 1.50 to 1.73 μm.

Studying the influence of sand, Gerbermann and Neher (1979) found that as the sand level increased from 0 to 100%, percent reflectance increased in the 0.44 to 0.86 μm region with increasing wavelength. Kristof et al. (1980) stated that reflectance curves for sand and silt contents showed a significant increase of reflected energy when the amount of sand and silt increased, and a distinct decrease in reflectance with increasing clay content. Stoner and Baumgardner (1980) observed that the reflectance in the 2.08 to 2.32 μm middle infrared band was negatively correlated with clay content, while it was positively correlated with fine and medium sand contents.

Organic Matter

Soil organic matter, consisting of decomposed residues and its constituents, are known to contribute strongly to soil reflectance. Many

studies have reported similar observations, suggesting that soil organic matter content is inversely related to the spectral reflectance. Obukhov and Orlov (1964) observed that as the humus content, the stable fraction of organic matter remaining after residue decomposition, gradually decreased down the soil profile, the spectral reflectance curve from 0.4 to 0.75 μm increased by a definite factor along the entire spectrum studied. This relationship was inherent to all soils where sesquioxides were uniformly distributed down the profile. The humic substance was more easily detected in the red region, 0.70 to 0.75 μm, than any of the other regions. Montgomery et al. (1976) found that the reflectance in the 0.6 to 1.1 μm range had the highest correlation with certain organic constituents, including nitrogenous compounds and humic acid fractions. Bowers and Hanks (1965) reported that the oxidation of organic matter by hydrogen peroxide increased the reflectance from all samples measured. The oxidized sample had a greater reflectance than did the check sample from 0.4 to 2.4 μm, but the difference beyond 1.8 μm became less identifiable. Matthews et al. (1973b) showed similar results in which the organic matter (12.8%) was destroyed in an Ellery silty clay soil. The removal of the organic matter increased the percent reflectance in the 0.5 to 1.15 μm region, while the reflectance decreased slightly from 1.15 to 2.6 μm.

Baumgardner et al. (1970) found that soils containing more than 2% organic matter content appeared to mask out the contributions of other soil parameters, whereas soils with less than 2% organic matter were harder to separate spectrally due to iron or manganese interference. Stoner and Baumgardner (1980) observed that when mineral soils were grouped into three levels of organic matter content, 0-3%, 3-5%, and 5-10%, the reflectance curves decreased with increasing organic matter content throughout the 0.52 to 2.32 μm wavelength region. Soils in the 5-10% organic matter range showed characteristics of the concave- shaped Type 1 curve, while soils in the 0-3% and 3-5% range followed the convex-shaped Type 2 curve pattern, recognized by Condit (1970). The Type 1 and Type 2 curves corresponded to high surface organic content Mollisols and lower surface organic content Alfisols and Ultisols, respectively.

Matthews et al. (1973b) reported that organic matter influenced reflectance from 0.5 to 1.2 μm, whereas Beck et al. (1976) recommended the 0.9 to 1.22 μm range best for determining soil organic carbon, which could in turn be related to organic matter content. Montgomery et al. (1976) found that organic matter content contributed significantly to variations in the visible region of the spectrum, while Krischnan et al. (1980) stated that no absorption band attributable to organic matter content was found in the infrared region from 0.8 to 2.4 μm, and the visible region provided better information for determining organic matter content in soils. Stoner and Baumgardner (1980) supported findings that reflectance in wavelengths up to 1.2 μm are the best for separating organic matter levels in soils. In addition, it was concluded that organic matter was the single most important variable in the visible and near infrared bands for explaining reflectance differences.

Iron Oxide

Investigating iron oxide reflectance in the visible range, Obukhov and Orlov (1964) observed that pure iron oxide exhibited a characteristic inflection at 0.53 to 0.58 μm, and that soil horizons with an elevated iron content could also be distinguished by an inflection in the region of 0.5 to 0.64 μm. Similar inflections were found in ferruginized quartz sand. After the iron compounds were removed from the sand by boiling in 10% hydrochloric acid, the inflection on the spectral reflectance curve disappeared entirely. These inflections were produced by iron oxide compounds which may form a film around individual particles of colorless minerals. They suggested that when iron was concentrated at the surface of aggregates (amorphous iron oxides) spectral brightness may be considerably lower than from the total content of iron compounds, including the amorphous and crystalline iron oxides.

Cihlar and Protz (1973) agreed that the free iron oxide deposited on the surface of peds and soil particles had a greater effect on spectral reflectance than the total iron oxide content. In their study relating the surface characteristics of soil mapping units to spectral reflectance, oxalate-extractable iron was preferred to dithionite-extractable iron. Schwertmann (1964) experimented with acid ammonium oxalate and varying light conditions, from darkness to ultraviolet light, and found that under the influence of light, crystallized iron oxides were brought into solution, whereas non-crystalline or amorphous iron oxides were soluble in the dark. The ratio between the oxalate-soluble fraction and the total free iron oxide (dithionite soluble) was named "degree of activity of iron oxides." The "active" fraction solubilized by an oxalate solution in the dark was considered more chemically reactive because of a greater specific surface area and inferior crystallinity, while those that required light for solubilization were more inert. McKeague and Day (1966) found that the oxalate extraction dissolved much of the iron and aluminum from the amorphous materials but very little from crystalline oxides, whereas the dithionite extraction dissolved a large proportion of the crystalline iron oxides as well as much of the amorphous materials. Raad et al. (1969) demonstrated that both sodium-dithionite and ammonium oxalate extractable iron, aluminum, and manganese in soils could be determined rapidly and accurately by atomic absorption spectroscopy without the removal of the extracting solution.

Matthews et al. (1973b) experimented with soil samples high in free iron oxide, the Hagerstown silt loam profile containing 4.2% iron oxide. The subsoils showed a strong absorption band at 0.9 μm, which was associated with high free iron oxide content. After the removal of the iron oxide, the reflectance showed a marked increase from 0.5 to 1.15 μm. In studying methods of computing the chromaticity of soils from the visible wavelengths, Karmanov (1970) observed that the reflection intensity of iron hydroxides containing little water and having a dark brown-red color increased most strongly from 0.554 to 0.596 μm, while iron oxides containing a large amount of water increased most from 0.5 to 0.54 μm. He also stated that the total reflectance of highly hydrated oxides was markedly higher than that of oxides

containing little water. Hunt et al. (1971b) studied the visible and near infrared spectra of various oxides and hydroxides. It was shown that spectral features, evidenced by bands or changes in the slope of the spectral curve, appeared as the result of either electronic oxidation states or vibrational processes in the hydroxyl groups or molecular water. Of the cations, iron was the most common source of electronic features. Typically, the ferrous ion produced the common band near 1.0 μm, while other ferrous bands were produced by transitions of iron near 0.55, 0.51, 0.45, and 0.43 μm. For the ferric ion, the major bands produced in the spectrum were results of transition near 0.87, 0.7 and 0.4 μm. A sharp absorption band from iron oxide occurred between 0.5 and 0.6 μm, but the presence of impurities may cause this edge to be sloped over an extended region. A closer spectral examination of brucite (magnesium hydroxide) showed a broad depression at about 0.9 μm due to iron impurities probably in both the ferrous and ferric state, which would also account for the steep fall-off near 0.45 μm. Stoner and Baumgardner (1980) observed the iron absorption bands either as well resolved dips in the reflectance curve or as broad features centered on specific wavelengths but extending their influence over a wide range of wavelengths. The ferric ion absorption band was characterized as a sharp inflection at 0.87 μm, whereas a broad band centered on 0.9 μm, extending over a 0.2 μm range, also indicated the presence of the ferric ion. In this study ranging from 0.52 to 2.32 μm, the ferrous iron absorption band was more difficult to identify. Close observation revealed evidence of the 1.0 μm ferrous ion band in several poorly drained soil samples. Comparison of duplicate Cecil soil samples having similar texture and organic matter content, but marked differences in free iron oxide content, revealed that the quantity of iron present in a soil appeared to affect the strength of the ferric iron absorption band. The soil sample with increased amounts of iron oxide exhibited a sharp absorption band at 0.9 μm, whereas the absorption band of the duplicate soil sample was difficult to identify.

Most correlations between iron oxide content and spectral reflectance remained low, but were much improved when samples were separated into the specific climatic zones where the soils were developed. Positive correlations with iron oxide content were found in the 0.62 to 0.72 μm and 0.82 to 0.92 μm regions of the spectrum. The middle infrared range, from 1.55 to 1.75 μm and 2.08 to 2.32 μm, negatively correlated with the iron oxide content. As previously stated, further investigation indicated that at least five general types of spectral reflectance curves could be identified based primarily on the presence or absence of probable ferric iron absorption bands at 0.7 and 0.9 μm. The curves were also based upon organic matter content and soil drainage characteristics.

Moisture Content

It can be observed that wetting a dry soil causes that soil to appear darker. Angstrom (1925) explained this darkening effect of moisture in soils on the internal total reflections within the thin water layer covering soil particles. A portion of the energy reflected from the soil surface would not

be reflected to space but would be re-reflected to the surface itself. Planet (1970) stated that the reflectance difference of a soil between its dry and wet states could be determined if several factors were taken into consideration: 1) variations in index of refraction of the water due to dissolved soil constituents, e.g., gypsum; 2) changes in the physical nature of the soil surface by the presence of water, e.g., compaction; and 3) the presence of materials whose reflectance properties are different from that of the soil in which they are located, e.g., rocks and vegetation.

Bowers and Hanks (1965) demonstrated a potential for measuring surface moisture content by the reflectance method and indicated the possibility of using wavelengths other than the water absorption bands. By using previously measured direct solar spectral distribution curves, one could acquire a reasonable indication of their potential effect in a field situation. By plotting reflectance against wavelength at several different moisture contents from 0.8 to 20.2% on a Newtonian silt loam soil, it was observed that at all wavelengths measured, reflectance decreased as the surface moisture content increased. Three water absorption bands were clearly identified, at 1.4, 1.9 and 2.2 μm, representing vibrational features due to free hydroxyl groups and molecular water (Hunt and Salisbury, 1970; Hunt et al., 1971b).

Obukhov and Orlov (1964) found that reflectivity decreased very strongly when the soil was wetted, yet the spectral curve did not change its appearance upon wetting. From the data obtained, they concluded that the spectral reflectance of soils under field conditions did not yield explicit results and a comparison of field and laboratory data was possible only if several constant conditions were observed: 1) an integration sphere was used and 2) the moisture content and degree of pulverization of the soil sample remained constant. Beck et al. (1976) conducted an experiment to determine how much of the variation in spectral reflectance could be explained by the water content. Subsamples from each soil in the study were equilibrated at two moisture tensions, 1/3 bar and 15 bars by the use of a pressure plate and pressure membrane apparatus, respectively. They showed that soil moisture at the 1/3 bar moisture tension level had the greatest influence on soil reflectance, especiallly at the absorption band at 1.9 μm. Since soils in the field cannot be measured at the same moisture content, reflectance in the 1.50 to 1.73 μm range was suggested as the best possibility for identifying water content in surface soils. Stoner and Baumgardner (1980) found the middle infrared band, 2.08 tO 2.32 μm, correlated best with moisture percentage by weight.

Stoner et al. (1979) also recognized that the extraneous contribution of soil moisture deriving from environmental factors should be controlled as much as possible. In their laboratory study of soil reflectance, a system capable of maintaining uniform moisture tension in soil samples was used. The equilibrium of soil moisture at one tension (1/10 bar) allowed the collection of spectral reflectance under conditions of a uniform tension. Since soils of different textures will hold different amounts of moisture at a given tension, this permitted the evaluation of differences in moisture contents as a factor influencing soil reflectance. Standard procedures for

laboratory study of soil reflectance allowed for comparison of soils from widely scattered sites with variables controlled to a greater extent than possible in the field (Stoner and Baumgardner, 1980).

MATERIALS AND METHODS

Site Selection

Within the state of Indiana sample sites were chosen according to their susceptibility to erosion. Aided by the SCS, sites were selected from different geographic locations, includng south central, west central and northeastern areas (Figure 1). The sites represented a variety of parent materials: loess over glacial outwash, lacustrine, calcareous loam till, and limestone residuum (Table 1). The soil orders common to Indiana, i.e., Mollisol, Alfisol and Ultisol, were represented in this study.

Field Sample Collection

Using map sheets and site locations provided by the SCS, soil samples were collected from topographic sequences exhibiting varying degrees of erosion. Using these maps, samples on the toposequence, excluding the depositional soil sample, were collected within the same soil catena boundary. Samples taken from the summit of the slope exhibited none to slight erosion, whereas the moderate to severely eroded soils were common on the shoulder and backslope, and the deposition at the toe of the slope (Figure 2). The degree of erosion was determined by the percentage of the original A horizon lost. The following classes were used:

None to Slight Erosion: less than 25% of the A horizon has been lost

Moderate Erosion: the plow layer consists of both A and B horizons

Severe Erosion: at least 75% of the A horizon has been lost

Deposit: recent accumulation usually of a different texture and/or color from the material directly underneath.

Soil samples were collected from the Ap horizon to a depth of about 15 cm (6") with a spade. Surface organic residue was removed prior to sampling and care was taken to preserve some of the peds for future color determination. Several kilograms of each sample were placed in labeled plastic bags, prior to preparation for laboratory analysis.

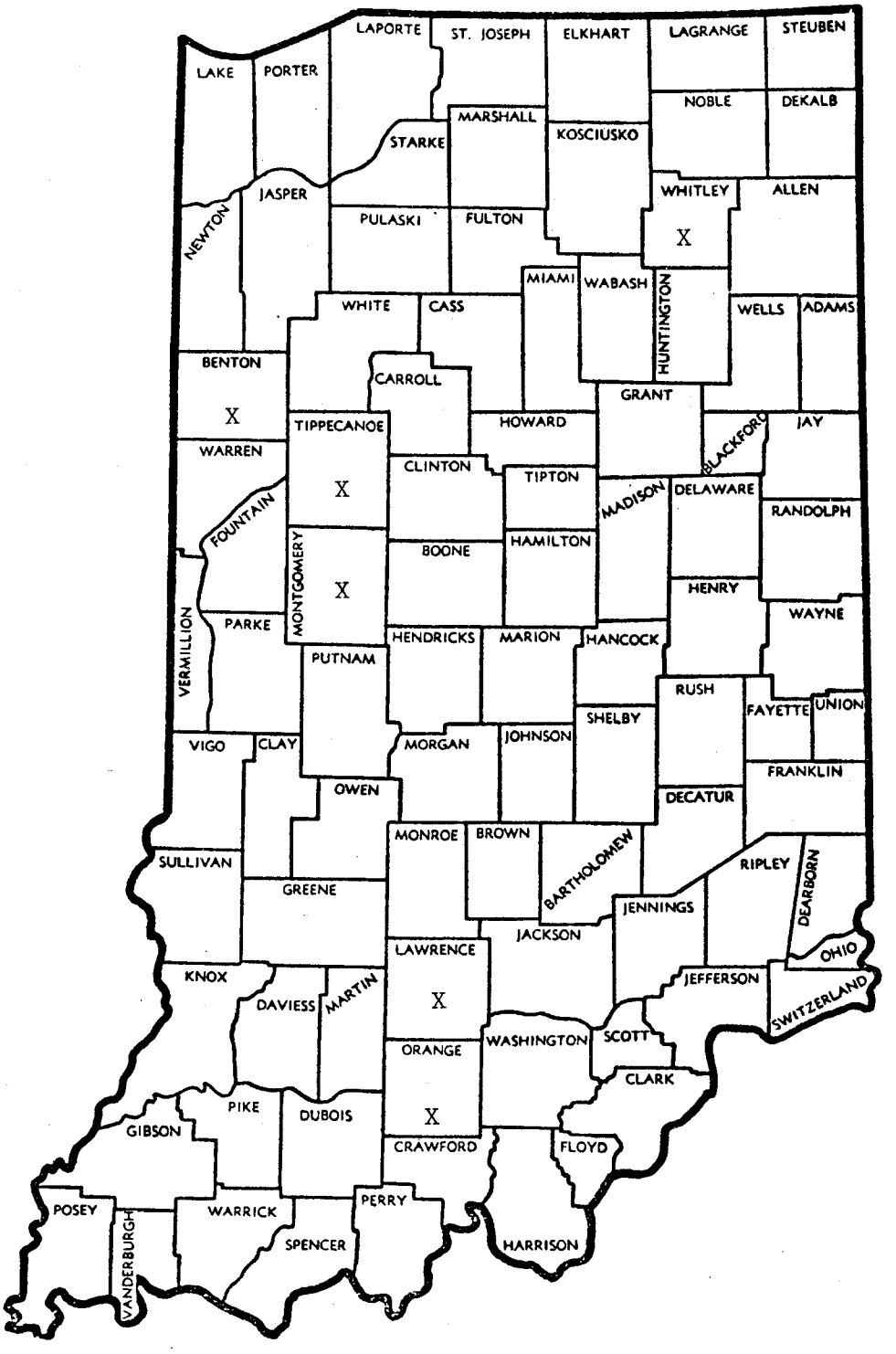

Figure 1. Map of Indiana delineating counties in which soil samples were collected.

Table 1. Soil series, parent material and taxonomic classification of six eroded toposequences and the Russell profile.

Soil Series	Parent Material	Classification
Sidell	loess over calcareous loam till (Wisconsin)	fine-silty, mixed Mesic Typic Arguidoll
Morley	loess over calcareous clay loam or silty clay loam till (Wisconsin)	fine, illitic mesic Typic Hapludalf
Miami	loess over calcareous laom till (Wisconsin)	fine-loamy, mixed mesic Typic Hapludalf
Bedford	loess over limestone residuum (Mississippian)	fine-silty, mixed mesic Typic Fraguidult
Frederick	loess over limestone residuum (Mississippian)	clayey, mixed mesic Typic Paleudult
Russell	loess over calcareous loam till (Wisconsin)	fine-silty, mixed mesic Typic Hapludalf

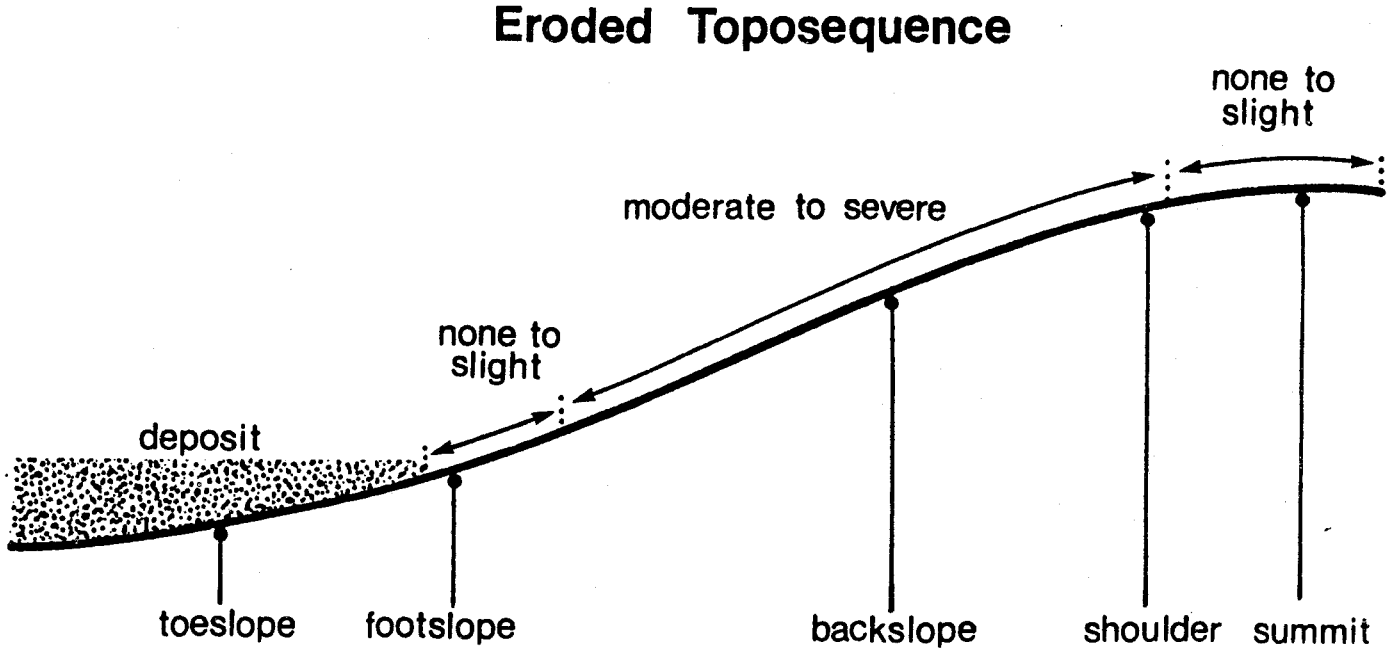

Figure 2. Toposequence with varying degrees of erosion.

For these samples collected from the topographic sequences, a numbering system described by Franzmeier et al. (1977) was used. An example of this system is S80IN-157-3-1, in which the S is the season the sample was collected (Summer), 80 is the year sampled (1980), and IN is the two-letter abbreviation of the state (Indiana). The next number is the county number (the alphabetical number of the county multiplied by two, minus one). Tippecanoe County is number 79 in an alphabetical list so the county number is (79 x 2) - 1, which equals 157. The next number represents the sequence of the soil sample; 3 states that it was the third sample collected. The final number represents the horizon sampled. All of the samples from the toposequences were taken from the Ap horizon and labeled one.

A second set of samples included in this study were from the Russell silt loam profile collected from the Agronomy Farm at Purdue University, West Lafayette, IN. A Giddings hydraulic probe truck was used to sample the profile to a depth of about 60 cm (24"). Each of the 15 cores had a constant volume of 456 cc (35.5 cubic inches) measured to an assimilated plow layer depth of 25 cm (10") with successive erosional losses of 2.5 cm (1") of topsoil per sample. Erosion classes of none to slight, moderate and severe were assigned to each sample according to the percentage of A horizon lost, as previously defined. Samples 1 to 4 were classified as none to slight, samples 5 to 9 as moderate and samples 10 to 15 as severe (Figure 3). The first core sampled was from about 0-25 cm (0-10") after the top 6-8 mm of surface vegetation was removed, the second from 2.5-27.5 cm (1-11"), the third from 5-30 cm (2-12"), until the final sample was taken from 35-60 cm (14-24"). Each sample was placed separately in a labeled plastic bag. This method of sampling permitted quantification of the percentages of each horizon existing in each sample.

Samples from the Russell profile were numbered according to the sequence of sampling of each 25 cm (10") core, i.e., the 5-30 cm (2-12") core sampled was the third sample taken. The Russell profile samples were not differentiated by horizonation because the sample often contained a mixture of several horizons.

Sample Preparation

Laboratory numbers were assigned to the field samples, and a subsample of the uniformly mixed soil was spread on a sheet of paper to dry. After several days, a kilogram of each air-dry sample was placed in storage for possible future study. Another kilogram of sample was prepared for laboratory analysis by crushing the soil with a wooden rolling pin, care being taken to destroy only the clods. This sample was passed through a 10 mesh screen to remove all particles larger than 2 mm in diameter.

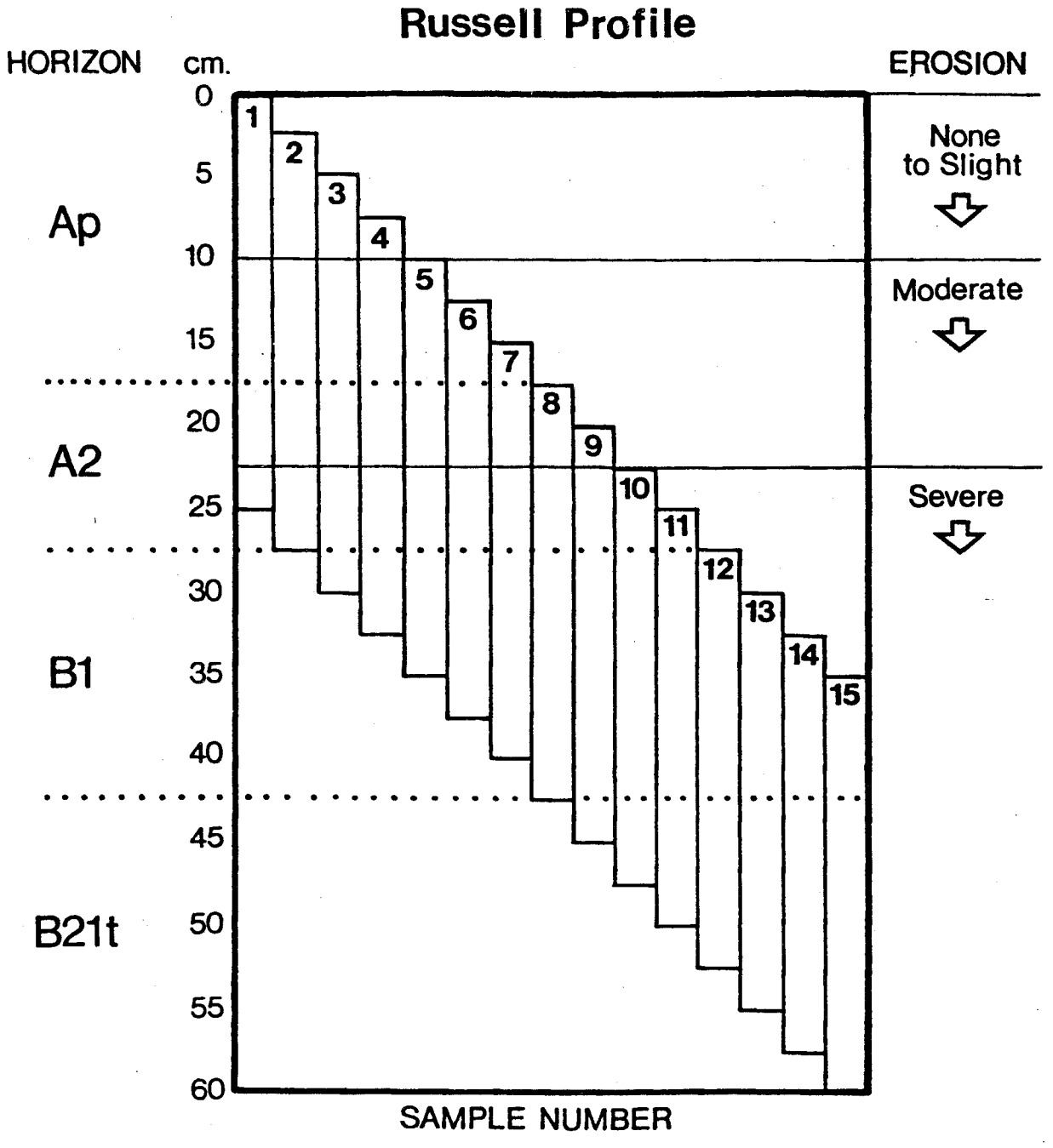

Figure 3. Sampling scheme for the Russell profile.

Chemical and Physical Analysis

Particle size distribution of organic matter-free soil was determined by the Soil Characterization Laboratory, Agronomy Department, Purdue University, using the pipette method (Franzmeier et al., 1977). Eight particle size fractions were measured on a percentage by weight basis: very coarse sand (2-1 mm), coarse sand (1-.5 mm), medium sand (.5-.25 mm), fine sand (.25-.10 mm), very fine sand (.10-.05 mm), coarse silt (.05-.02 mm), fine silt (.02-.002 mm) and clay (.002 mm).

Organic carbon was measured by the Mebius method, using soil samples that had been ground and passed through a 100 mesh sieve. The organic matter was oxidized by chromic acid plus external heat. This method assumes complete digestion of the organic carbon. The excess chromic acid is determined by titration with ferrous ammonium sulfate and the oxidized organic carbon is calculated from the amount of chromic acid reduced (Franzmeier et al., 1977). A check sample was included in each run and duplicates of each sample were run on different days, then averaged. Organic matter was estimated by multiplying the percent organic carbon by 1.72.

The method used to measure the amount of free iron oxide in the soil, including the amorphous coatings and the crystalline iron oxide, was a citrate-bicarbonate-dithionite (CBD) analysis. The iron is reduced by sodium dithionite, buffered by sodium bicarbonate and chelated by sodium citrate. A colorimetric reading at 510 nm was used to determine the amount of free iron oxide. The CBD supernatant was also used to measure the aluminum oxide content in the soils, utilizing an atomic absorption spectrophotometer with a nitrous oxide air-acetylene flame at 309.3 nm (Franzmeier et al., 1977).

An acid ammonium oxalate solution was used for the extraction of the non-crystalline or amorphous iron oxide. The oxalate solution was adjusted to pH 3.0 to increase the rate of the iron reduction. Twenty-five mls of 0.2 M acid ammonium oxalate solution were added to a 200 mg soil sample which had been ground and passed through a 100 mesh sieve. The sample and solution were shaken in tightly closed, plastic centrifuge tubes, lying horizontally in a closed box, for three hours. The closed box prevented any light from influencing the reaction, and in this manner allowed only the amorphous compounds (including the iron bound to organic matter) to react with the oxalate, while avoiding any precipitation of the ferrous oxalate compound. The amorphous iron oxide content was determined using the undiluted filtrate at 372 nm on the atomic absorption (AA) spectrophotometer (Schwertmann, 1964; Raad et al., 1969; Miller, 1981). The iron oxide ratio of total iron oxide (CBD-soluble) to amorphous iron oxide (oxalate-soluble) was calculated.

Cation exchange capacity (CEC) expressed in terms of milliequivalents per 100 g of soil was determined by the summation of the exchangeable basic cations of Ca^{++}, Mg^{++}, and K^{+} plus the exchangeable acidity. Soil samples were ground and passed through a 60 mesh sieve. The adsorbed cations were

displaced with a concentrated ammonium acetate solution, and the leachate containing these cations was analyzed using an AA. Since sodium content in most Indiana soils is insignificant, only Ca, Mg and K were analyzed. Extractable acidity was determined by leaching the soil with a barium chloride-triethanolamine ($BaCl_2$-TEA) solution. The acidic cations are replaced and hydrolyzed by the barium while the TEA neutralized the dissociated acidic groups on the clay surface. The leachate was titrated with hydrochloric acid and the amount of hydrogen calculated (Franzmeier et al., 1977).

Color of the soil samples was determined in the bright sunlight on a dry and moist basis with the use of a Munsell color chart. Peds from the original field samples were read for both dry and moist color on the topographic sequence samples. To obtain a more uniform color designation for the 25 cm core samples, color was determined from the 2 mm diameter samples. Variations in color were quite pronounced depending on which section of the core was used; therefore, a uniform mixture of the soil was sampled for color determination. Duplicate color readings were recorded on all samples.

A standardized procedure for preparing soil samples for spectral reflectance measurements (Stoner and Baumgardner, 1980) was used. A modified version of the soil moisture tension table described by Leamer and Shaw (1941), consisting of a plexiglass-framed tension table capable of holding 28 soil samples, was used (Figure 4a). The blotter paper was replaced with a more durable asbestos membrane (Jamison and Reed, 1949). In order to avoid external variations due to evaporation or contaminants from the environment, a plexiglass top covered the soil samples, yet did not interfere with the atmospheric pressure on the upper membrane.

Sample holders, as designed and described by Stoner and Baumgardner (1980), fit the specifications of the spectroradiometer field of view and the tension table operating principle. Plastic sample rings, painted non-reflecting black to reduce unwanted reflectance, with a 10 cm inside diameter and 2 cm depth, provided sufficient circumference and depth to assure that only the soil was being viewed. A 60 mesh brass strainer cloth was stretched taut across the sample ring, as it was necessary to provide contact between the soil and the asbestos membrane. Filter paper was placed under each sample to protect the membrane.

A representative soil sample was transferred into the sample holders and leveled; care was taken to avoid segregation by particle size. The soil samples were saturated with deionized water from the bottom. This method allowed the micro-pore spaces to be completely filled with water. After four hours of saturation, the samples were placed on the tension table for 24 hours to assure equilibration (Stoner and Baumgardner, 1980). Samples were transferred from the tension table to a horizontal platform to measure the reflectance and immediately placed back on the tension table. The moisture content was determined for each of the soil samples after equilibration at 0.1 bar tension immediately after collecting the spectral reflectance. A subsample was removed from each holder approximating the area viewed by the spectroradiometer to a depth of 1 cm. These samples were weighed, oven-dried at 105 C for 24 hours, and reweighed to determine percent moisture by weight.

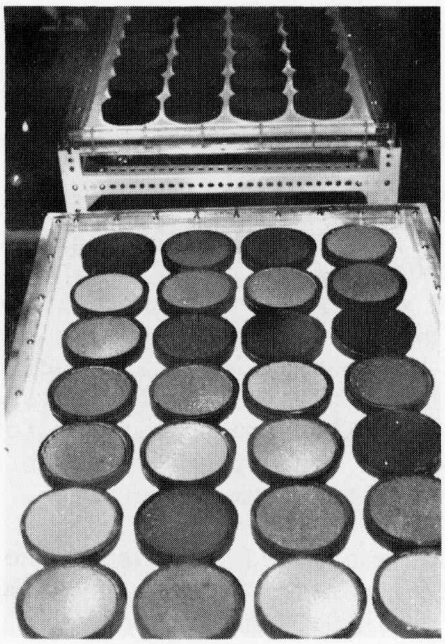

a. Fifty-six soil samples ready for spectral measurement after 24 hours equilibration at 100 cm H_2O tension.

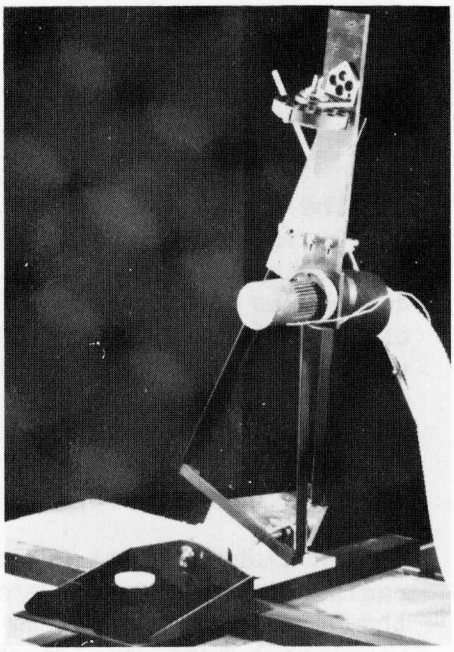

b. BRF reflectometer positioned for soil sample detection by the Exotech 20C spectro-radiometer.

Figure 4. Setup for laboratory spectral measurements of soils. (Reprinted from Stoner and Baumgardner, 1980)

Since the tension table could accommodate 28 soil samples at one time, each run included two check samples randomly placed on the tension table. Duplicates of soil samples were also run on separate days; a total of 55 soil samples were analyzed.

Bidirectional Reflectance Factor

The measurement method used to obtain bidirectional reflectance factor (BRF) is based upon the utilization of a perfectly diffuse, completely reflecting surface as a reference (Silva, 1978). Reflectance factor is defined as the ratio of flux reflected by a target under specified conditions of irradiation and viewing to that reflected by an ideal, completely reflecting, perfectly diffuse surface, identically irradiated and viewed (Figure 5). "Perfectly diffuse" means that the surface reflects equally in all directions. The radiance of a uniformly illuminated surface (of infinite extent) is constant for any viewing angle. "Completely reflecting" means that all of the flux on the surface is reflected from the surface.

An Exotech Model 20C spectroradiometer was used to measure the reflected radiance from prepared soil samples (Figure 4b). Spectral readings covered the wavelength range from 0.52 to 2.32 μm in 0.01 μm increments. The short wavelength head of the spectroradiometer contains two detectors, a silicon detector covering the wavelength from 0.35 to 0.70 μm and the lead sulfide detector, which uses a circular variable filter (CVF) to cover two wavelength ranges, 0.65 to 1.13 μm and 1.25 to 2.5 μm (Silva et al., 1971). The spectroradiometer depends on an external source for its illumination, a 1000 watt tungsten iodine coiled filament lamp, mounted in a light, tight air-cooled housing. The lamp irradiates the sample at one solar constant level in a collimated directional (from normal to 45^{o}) manner (DeWitt and Robinson, 1976). The sensing head of the spectroradiometer is mounted in a vertical fixed position approximately 2.4 m above the sample stage.

Pressed barium sulfate calibration standard was measured every fifth sample to measure any variations within the instrument or illumination source. Six complete scans from 0.52 to 2.32 μm were taken of each sample and averaged when the data were digitized and processed.

Data Logging and Analysis of Reflectance Curves

All the data collected from each soil sample were recorded on information cards and stored together with the spectral reflectance measurements on the digital computer tape at LARS. This provided instant retrieval of all information, including summaries of data, the ability to graph the spectral curves alone or in relationship to specific soil parameters, and perform statistical analysis on the data with the spectral values.

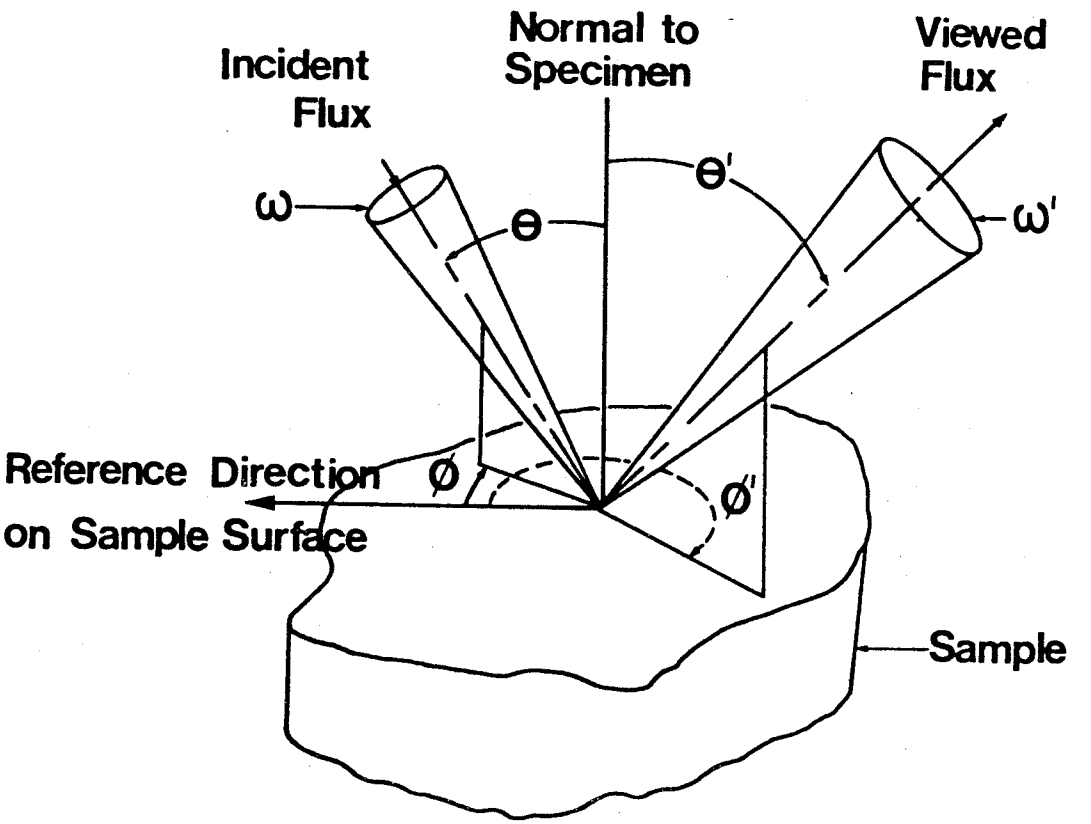

Figure 5. Geometric parameter describing reflection from a surface: θ = zenith angle, ϕ = azimuthal angle, ω = beam solid angle,sr. A prime on a symbol refers to viewing (or reflected) conditions. (Reprinted from DeWitt and Robinson, 1976)

In order to observe simulated spectral curves of Landsat, the mean value of the soil reflectance data (% mean BRF) was computed and plotted in the four Landsat bands. The four Landsat bands include two bands in the visible region (from 0.5 to 0.6 μm and 0.6 to 0.7 μm) and two bands in the near infrared region (from 0.7 to 0.8 μm and 0.8 to 1.1 μm). These graphs could be useful for making comparisons between the laboratory and expected satellite spectral data.

The reflectance data were divided into twelve spectral bands from 0.52 to 2.32 μm for a correlation study of nine soil parameters (Table 2). Bands 1 to 8 all have 0.1 μm band widths. Bands 1 and 2 cover the visible wavelength region; bands 3 to 8 include the near infrared region; and bands 9 to 12 are middle infrared bands. Bands 9 and 11 cover the region of known water absorption. Bands 1 to 6 cover the same spectral range as the four existing bands of the Landsat multispectral scanner. Bands 10 and 12 are proposed Thematic Mapper bands with band 12 being slightly altered by the cutoff of the spectroradiometric data at 2.32 μm (Stoner and Baumgardner, 1980).

Simple correlation coefficients were calculated between nine soil parameters and reflectance in 12 wavelength bands. The nine soil parameters studied were organic carbon content, total iron oxide content, amorphous iron oxide content, the iron oxide ratio, sand, silt, and clay content, cation exchange capacity and percentage moisture by weight. Correlation coefficients and their probability were computed in each of the twelve bands and recorded in order of highest to lowest correlation by soil parameter. As sample sizes became smaller, the 95% confidence intervals on the correlation coefficients became broader.

A two-factor analysis of variance with missing values was calculated for six toposequences and four erosion classes. The four erosion classes were none, moderate, severe, and deposition. Soils classified as slightly eroded were grouped with those of moderate erosion and the very severely eroded with the severe class to decrease spaces with missing values and thus increase the significance of the analysis. Fourteen dependent variables were analyzed. In addition to the nine soil parameters used in the correlation study, the logarithm of organic carbon content and the four Landsat bands were included. Tukey's test of nonadditivity was performed to show which toposequences and/or erosion classes differed from each other.

Analysis of the standardized response ratio of the toposequences was performed on the spectral reflectance curves from 0.52 to 2.32 μm. The reflectance of each spectral curve was divided by the reflectance of the non-eroded soil in the individual toposequences. This procedure allowed comparison of the eroded and depositional response ratios to the non-eroded "standard" curve, enhancing the convex and/or concave shape of the curve in relation to the standard (Vanderbilt, 1981).

A polynominal regression was performed on the standardized response ratio at 59 wavelengths covering 0.01 μm intervals from 0.52 to 1.1 μm. Coefficients of the second-degree term were used for comparisons of shape and degree of curvature of the eroded and depositional spectral response ratio in relation to the non-eroded standard.

Table 2. Spectral reflectance bands used in analysis.

Band	Wavelength (μm)	Spectral Range
1	0.52 - 0.62	visible
2	0.62 - 0.72	visible
3	0.72 - 0.82	near IR
4	0.82 - 0.92	near IR
5	0.92 - 1.02	near IR
6	1.02 - 1.12	near IR
7	1.12 - 1.22	near IR
8	1.22 - 1.32	near IR
9	1.42 - 1.48	middle IR
10	1.55 - 1.75	middle IR
11	1.92 - 1.98	middle IR
12	2.08 - 2.32	middle IR

RESULTS AND DISCUSSION

Chemical and Physical Properties

The results of the chemical and physical analyses of the toposequences are listed in Table 3. A summary of selected data is listed in Table 3a comparing the soil parameters most strongly influenced by the degree of soil erosion, i.e., clay, organic matter and the various forms of iron oxide.

In the Sidell (Montgomery), Miami and Bedford toposequences the clay content of each changed only slightly with the erosion class. In the Morley and Frederick toposequences clay content increased with the severity of erosion. The depositional soils were equal to or slightly higher in clay content than the non-eroded soils, with the exception of the Morley toposequence.

As would be expected percent organic matter for each of the soils was highest in the depositional soils followed by the non-eroded, slightly eroded and severely eroded soils. An exception to this was observed in the Bedford and Frederick toposequences where the organic matter of the moderately eroded soil and the severe and very severely eroded soils of the respective toposequences was as high or higher than the organic matter in the non-eroded and depositional soils.

In all of the toposequences except the Sidell (Benton), the total iron oxide content is nearly equal to or higher in the eroded soils than in the non-eroded and depositional soils. The Sidell (Montgomery), Morley, Miami and Frederick toposequences increase in total iron oxide as the degree of erosion increases. The Sidell (Benton) toposequence decreases in total iron oxide as erosion becomes more severe.

The amorphous iron oxide content was equal to or higher in the non-eroded and depositional soils, correlating with the results of the organic matter. As observed previously, the Frederick toposequence was the exception. The amorphous iron oxide decreased with increased erosion in the Sidell, Morley and Bedford toposequences.

In all toposequences the iron oxide ratio was higher in the eroded soils than the non-eroded soils. Higher values of the iron oxide ratio observed in the depositional soils of the Sidell (Benton) and Frederick toposequences may be the result of recent accumulation of currently eroding soils. With the exception of the Miami toposequence, the iron oxide ratio increases with the severity of erosion.

The results of the Russell silt loam profile are shown in Table 4. With increasing depth in the soil profile the organic matter content, cation exchange capacity and sand content decrease; the clay content, iron oxide

Table 3. Chemical and physical data of the soil parameters for the eroded toposequences.

Topo-sequence	County	Erosion	Texture	Sand %	Silt %	Clay* %	OM %	CEC	pH	Total Fe_2O_3 %	Amorphous Fe_2O_3 %	Total: Amorphous Ratio	Total Al_2O_3 %	Moisture %	Color (Moist)
Sidell	Benton	None	SiL	32	52	16	2.8	17	5.7	.85	.41	2.07	.20	29	10YR 3/2
		Moderate	L	49	41	10	1.9	10	6.1	.66	.27	2.44	.14	24	10YR 4/3
		Severe	FSL	61	30	9	1.7	9	6.0	.62	.25	2.48	.14	19	10YR 3/3
		Deposit	SiL	29	52	19	3.4	24	5.6	.94	.32	2.94	.21	30	10YR 2/1
Sidell	Mont-gomery	None	SiL	11	68	21	2.8	20	6.0	1.18	.43	2.74	.22	33	10YR 3/2
		Slight	SiL	15	62	23	2.2	21	6.0	1.41	.43	3.28	.28	27	10YR 3/3
		Severe	L	33	44	23	2.2	19	6.5	1.55	.37	4.19	.26	22	10YR 3/3
		Deposit	SiL	10	69	21	3.3	22	5.2	1.09	.55	1.98	.27	34	10YR 3/2
Morley	Whitley	None	L	37	46	17	2.6	16	6.3	1.07	.38	2.82	.19	28	10YR 3/3
		Moderate	L	37	42	21	2.1	15	5.2	1.22	.31	3.94	.20	24	10YR 4/3
		Severe	CL	43	27	31	1.7	21	7.7	1.75	.29	6.03	.21	22	10YR 4/3
		Deposit	FSL	55	30	15	2.8	16	5.6	.88	.31	2.84	.15	19	10YR 3/2
Miami	Mont-gomery	Slight	SiL	32	54	14	1.4	12	4.7	.96	.25	3.84	.17	26	10YR 4/3
		Moderate	SiL	17	62	21	1.2	18	4.8	1.36	.44	3.09	.23	28	10YR 4/4
		Severe	L	50	30	21	1.2	15	5.2	1.40	.25	5.60	.22	21	10YR 3/4
		Deposit	SiL	33	53	14	1.7	15	4.9	1.02	.45	2.27	.20	26	10YR 3/3
Bedford	Orange	None	SiL	7	79	15	1.7	12	5.4	1.15	.22	5.23	.29	30	10YR 4/4
		Slight	SiL	8	74	19	1.4	15	4.9	1.54	.20	7.70	.32	28	10YR 4/4
		Moderate	SiL	8	75	17	1.9	14	6.0	1.36	.17	8.00	.29	32	10YR 5/4
Fred-erick	Law-rence	None	SiL	2	79	19	1.7	14	6.5	1.33	.17	7.82	.25	31	10YR 4/4
		Moderate	SiL	3	71	26	1.5	18	6.1	2.13	.23	9.26	.34	28	10YR 4/5
		Severe	SiCL	5	66	29	2.1	18	6.3	2.19	.15	14.60	.36	31	7.5YR 4/6
		V. Severe	SiCL	7	55	38	1.9	21	6.7	3.16	.20	15.80	.41	30	5YR 4/6
		Deposit	SiCL	6	67	27	1.9	18	6.8	2.14	.22	9.73	.33	30	10YR 4/4

* % sand, silt and clay rounded up

Table 3a. Chemical and physical data of selected soil parameters for the eroded toposequences.

% Clay	Sidell (B)	Sidell (M)	Morley	Miami	Bed-ford	Fred-erick
Deposit	19	21	15	14	-	27
None	16	21	17	-	15	19
Slight	-	23	-	14	19	-
Moderate	10	-	21	21	17	26
Severe	9	23	31	21	-	29
Very Severe	-	-	-	-	-	38
% O.M.						
Deposit	3.4	3.3	2.8	1.7	-	1.9
None	2.8	2.8	2.6	-	1.7	1.7
Slight	-	2.2	-	1.4	1.4	-
Moderate	1.9	-	2.1	1.2	1.9	1.5
Severe	1.7	2.2	1.7	1.2	-	2.1
Very Severe	-	-	-	-	-	1.9
% Total Iron Oxide						
Deposit	.94	1.09	.88	1.02	-	2.14
None	.85	1.18	1.07	-	1.15	1.33
Slight	-	1.41	-	.96	1.54	-
Moderate	.66	-	1.22	1.36	1.36	2.13
Severe	.62	1.55	1.75	1.40	-	2.19
Very Severe	-	-	-	-	-	3.16
% Amorphous Iron Oxide						
Deposit	.32	.55	.31	.45	-	.22
None	.41	.43	.38	-	.22	.17
Slight	-	.43	-	.25	.20	-
Moderate	.27	-	.31	.44	.17	.23
Severe	.25	.37	.29	.25	-	.15
Very Severe	-	-	-	-	-	.20
Iron Oxide Ratio						
Deposit	2.94	1.98	2.84	2.27	-	9.73
None	2.07	2.74	2.82	-	5.23	7.82
Slight	-	3.28	-	3.84	7.70	-
Moderate	2.44	-	3.94	3.09	8.00	9.26
Severe	2.48	4.19	6.03	5.60	-	14.60
Very Severe	-	-	-	-	-	15.80

Table 4. Chemical and physical data of the soil parameters for the Russell profile.

Russell Sample #	Erosion	% Ap: A2: B1: B21t	Texture	% Sand	Silt	Clay*	OM	CEC	pH	% Total Fe_2O_3	Amorphous Fe_2O_3	Total: Amorphous Ratio	% Total Al_2O_3	Moisture	Color (Moist)
1	None-Slight	70:30	SiL	13	73	15	2.9	17	5.5	.71	.41	1.73	.17	37	10YR 3/2
2	None-Slight	60:40	SiL	12	74	14	2.2	16	5.6	.79	.42	1.88	.20	35	10YR 4/3
3	None-Slight	50:40:10	SiL	12	74	15	1.5	14	5.7	.78	.41	1.90	.14	33	10YR 4/3
4	None-Slight	40:40:20	SiL	11	73	16	2.0	14	5.8	.78	.40	1.95	.13	33	10YR 3/3
5	Moderate	30:40:30	SiL	9	74	17	1.4	14	5.8	.86	.40	2.15	.13	32	10YR 4/3
6	Moderate	20:40:40	SiL	9	74	17	1.4	16	5.7	.90	.44	2.05	.15	33	10YR 4/3
7	Moderate	10:40:50	SiL	8	73	19	1.0	14	5.7	.99	.41	2.41	.16	32	10YR 4/3
8	Moderate	40:60	SiL	8	73	19	.9	15	5.8	.98	.40	2.45	.16	32	10YR 5/4
9	Moderate	30:60:10	SiL	7	71	22	.7	16	5.8	1.18	.44	2.68	.16	31	10YR 4/4
10	Severe	20:60:20	SiL	7	68	25	.9	18	5.7	1.18	.45	2.62	.17	33	10YR 4/4
11	Severe	10:60:30	SiL	7	68	25	.9	19	5.8	1.29	.45	2.87	.18	32	10YR 4/4
12	Severe	60:40	SiL	7	68	25	.7	20	5.7	1.34	.47	2.85	.19	32	10YR 4/4
13	Severe	50:50	SiCL	7	65	29	.7	23	5.7	1.44	.48	3.00	.21	34	10YR 4/4
14	Severe	40:60	SiCL	7	67	27	.9	22	5.8	1.43	.44	3.25	.20	34	10YR 4/6
15	Severe	30:70	SiCL	8	64	28	.7	22	5.7	1.51	.44	3.43	.21	35	10YR 4/6

* % sand, silt and clay rounded up

content and iron oxide ratio increase; and the silt and amorphous iron oxide content remain nearly constant. A transitional zone appears between samples 7 and 8 where the soil parameters change very little. From sample 9 down the remainder of the profile sampled, the organic matter and sand content remain fairly constant, silt content decreases, and clay content, cation exchange capacity and iron oxide compounds increase.

Spectral Reflectance Curves

Repeatability

Figure 6 plots the % BRF of the four replicate check samples against the wavelength from 0.52 to 2.32 μm. Reflectance of the check sample varied little between the two samples measured on the same day or among the samples measured on different days. The moisture percentage by weight differed by 13% relative to the average content of 28.3% moisture of the four check samples.

Additional soil samples were duplicated for spectral reflectance measurements on different days (Figures 7 and 8). A 9% difference in moisture relative to an average of 31.7% was calculated for the non-eroded Sidell subsamples while a difference of less than 2% moisture relative to a 27.8% average moisture was measured for the moderately eroded Miami toposequence subsamples. Repeatability of the spectral measurements was demonstrated by randomly placing replicate samples on the tension table. This was observed even in circumstances where the moisture content of the soil samples differed slightly.

During analysis of the spectral curves, it was impossible to place importance on the erratic inflections greater than 0.8 μm. These irregularities were due to a high gain setting in the instrumentation resulting in a low signal-to-noise ratio and high noise reflectance data. Discussion will be limited to the general curve shape.

Curve Types

Figure 10 graphs the percentage of bidirectional reflectance factor as a function of wavelength for the Sidell toposequence sampled in Benton County, Indiana. The curve shapes of the uneroded (non-eroded and depositional) soils are characteristic of the Type 1 curve of certain Mollisols as described by Stoner and Baumgardner (1980) in Figure 9. Both curves of the uneroded soils have a concave shape from 0.52 to 1.0 μm. The curves then become linear with slightly less positive slope from 1.0 to 1.3 μm. The curve shape of the moderately eroded soil resembles the Type 2 convex-shaped curve. It shows a positive and increasing rate of change in the visible wavelengths to about 0.7 μm with a slight inflection from 0.53 to 0.58 μm. The slope increases from about 0.7 to 0.86 Um, becomes negative or zero from 0.82 to 0.86 μm and decreases to 1.3 μm. Several dips are noticeable in the near infrared at 0.9 and 1.2 μm. The curve of the severely eroded soil

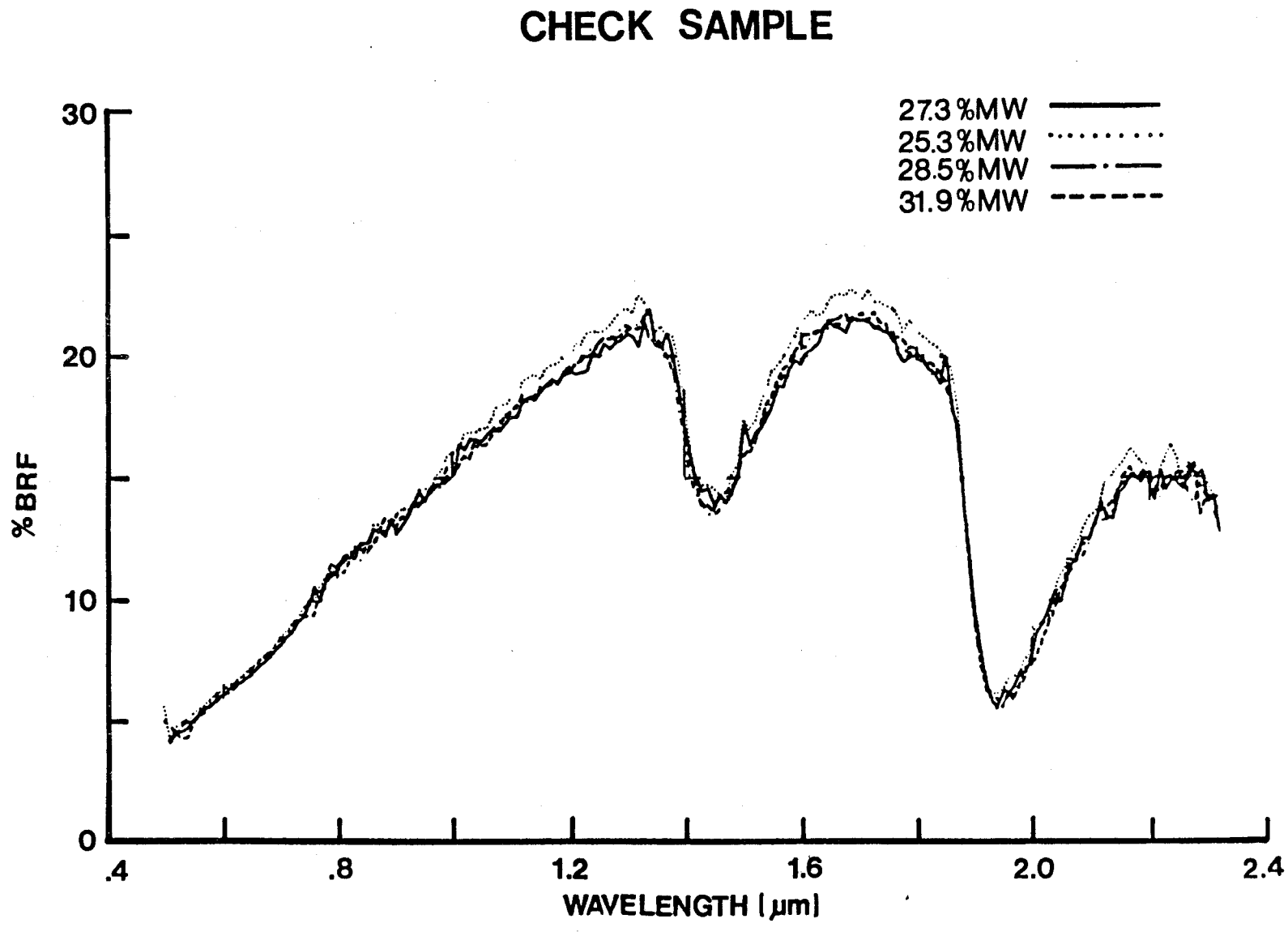

Figure 6. Reflectance curves for the four replications of the check sample.

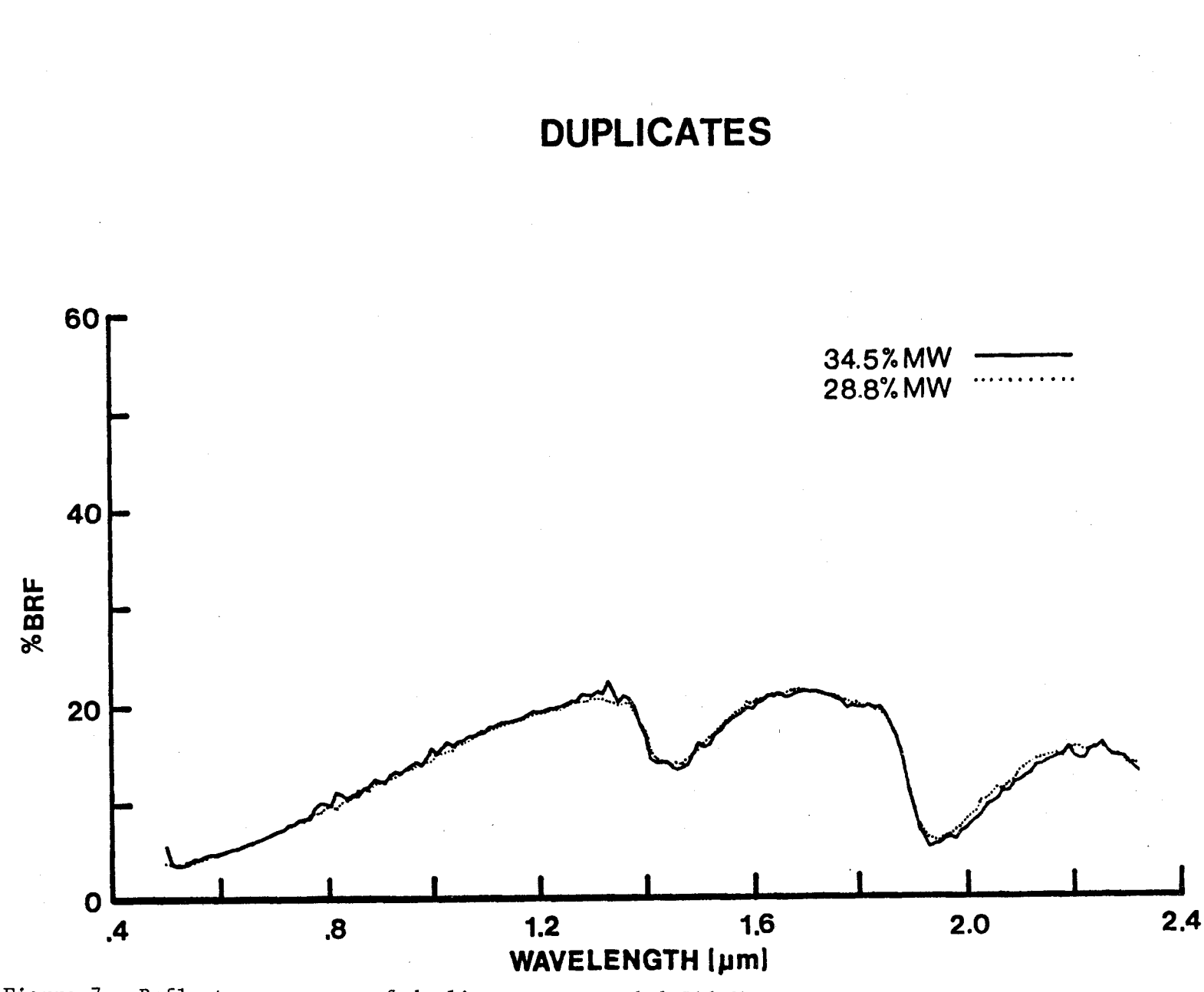

Figure 7. Reflectance curves of duplicate, non-eroded Sidell toposequence samples.

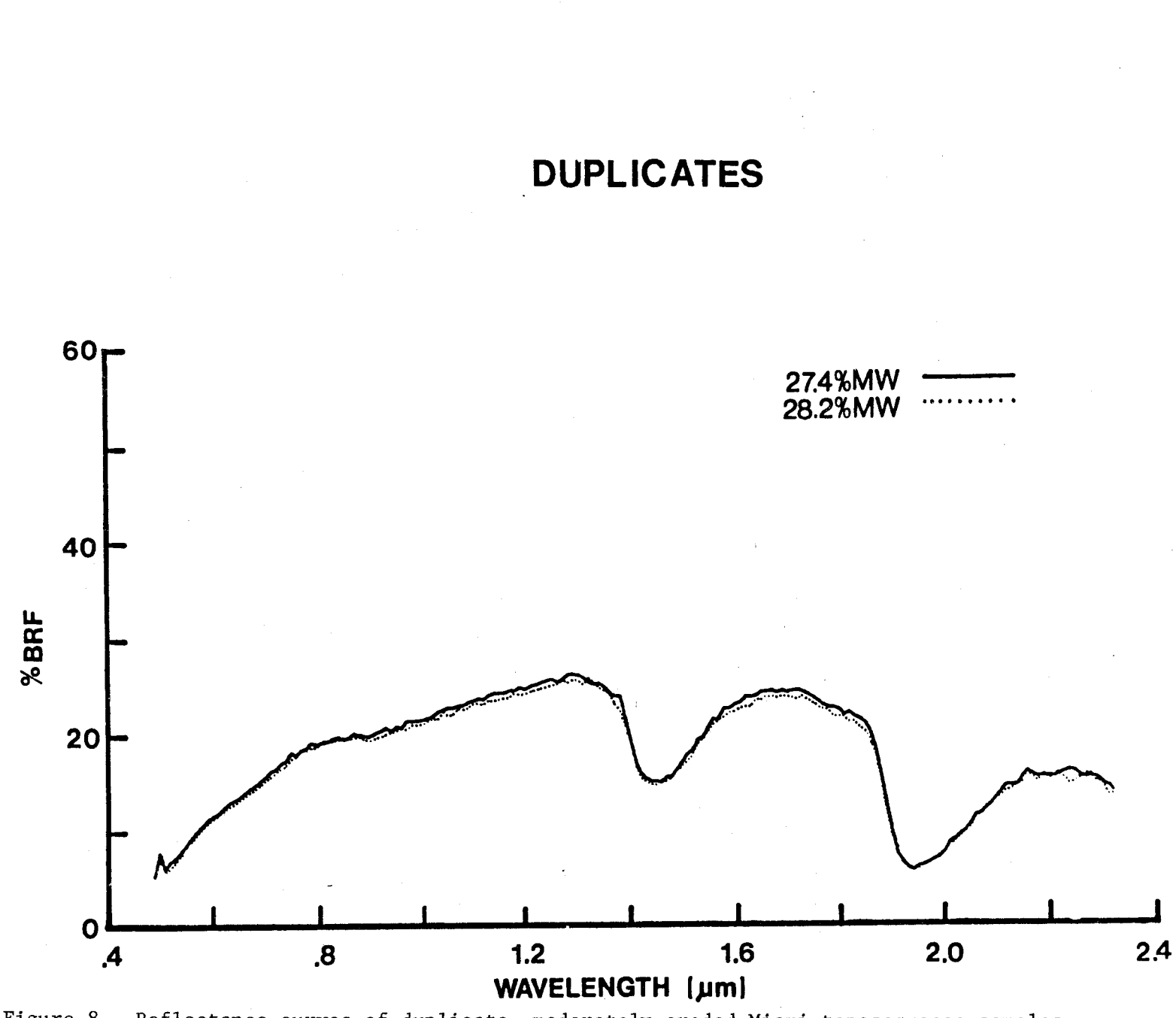

Figure 8. Reflectance curves of duplicate, moderately eroded Miami toposequence samples.

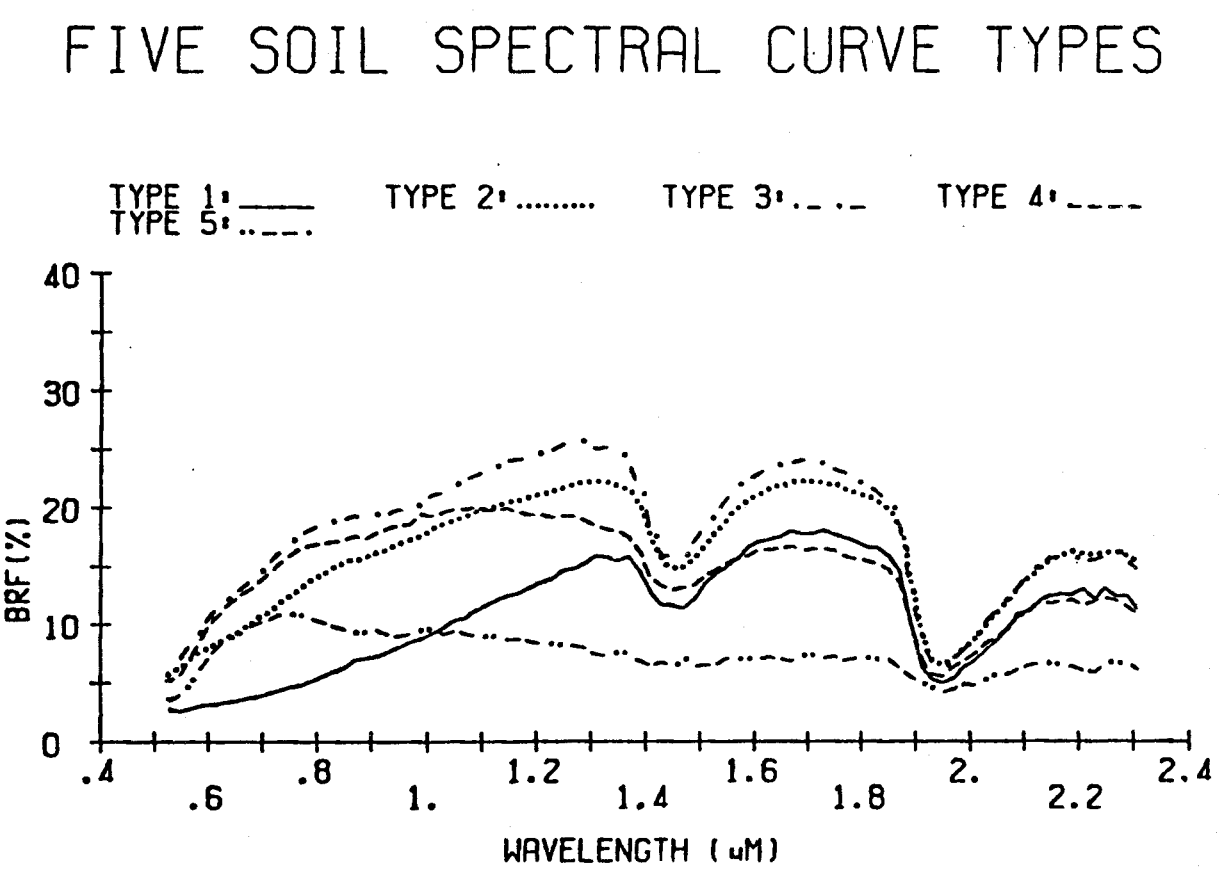

Figure 9. Five spectral reflectance curve types described by Stoner and Baumgardner, 1980.

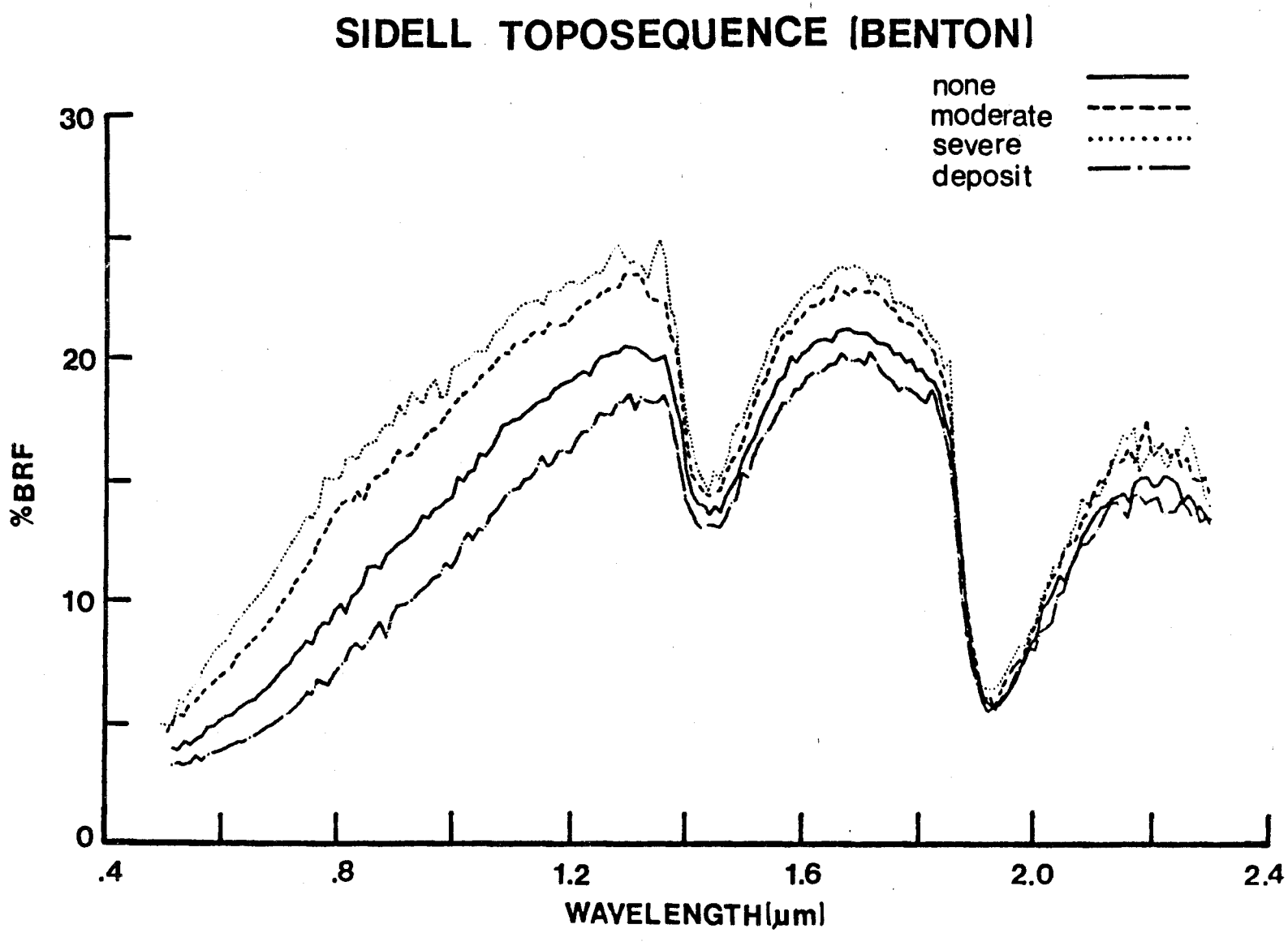

Figure 10. Reflectance curves of an eroded Sidell toposequence.

increases until a dip at 0.55 μm and remains constant to 0.77 μm. The general function of the curve decreases with many irregular peaks and inflections until 1.3 μm resembling the Type 2 curve shape. The severely eroded soil curve has the highest reflectivity, the moderate is second, the non-eroded is third and the depositional curve reflects the least of the samples in this toposequence.

Figure 11 is an example of the standardized bidirectional response ratio plotted as a function of wavelength for the eroded Sidell toposequence. The non-eroded spectral curve was previously defined as the standard and its response ratio equals one. The ratio curve of the depositional soil is concave to about 1.4 μm with nearly zero slope to 1.9 μm relative to the standard. The curvature of the severely eroded soil ratio is more convex than that of the moderately eroded soil ratio; both are nearly zero from 0.55 to 0.8 μm and concave to 1.4 μm. The response ratio is highest in the severely eroded soil and lowest in the depositional soil. The non-eroded standard curve separates the eroded from the uneroded soil ratios up to 1.9 μm with the largest degree of separation from 0.55 to 0.9 μm.

Figure 12 graphs the spectral reflectance of a Sidell toposequence from Montgomery County, Indiana. The non-eroded and depositional concave-shaped curves resemble those described in Figure 10. The curves of the slightly and severely eroded soils are difficult to separate in the visible and near infrared wavelengths until 0.78 μm. Their convex-shaped curves resemble Type 2 curves, decreasing to about 0.62 μm and remaining constant from 0.68 to 0.78 μm. A leveling of the slightly eroded soil curve is noticeable in the near infrared 0.82 to 0.9 μm range even though both curves show numerous peaks in the near infrared region from 0.8 to 1.30 μm as the slope decreases. The reflectance of the slightly eroded soil curve is higher than the severe from 0.78 μm. In this toposequence the eroded soils reflect more than the non-eroded and depositional soils, respectively.

Figure 13 is an example of an simulated Landsat spectral reflectance graph for the Sidell toposequence. The four Landsat bands range from 0.5 to 1.1 μm, including two bands in the visible region (0.5 to 0.6 μm and 0.6 to 0.7 μm) and two bands in the near infrared region (0.7 to 0.8 μm and 0.8 to 1.1 μm). The uneroded soil curves are concave-shaped and increase in slope. The curve of the slightly eroded soil is somewhat concave and increases in bands 1 to 3 while decreasing in slope in band 4. The severely eroded soil curve is the most reflective in this toposequence in bands 1 and 2 then undercuts the slightly eroded soil curve around band 3. The curves of the eroded soils are more highly reflective than the curves of the uneroded soils. The depositional soil curve is the least reflective of this toposequence.

Figure 14 measures the spectral reflectance curves for the Morley toposequence collected from Whitley County, Indiana. The curves of the uneroded soils appear to be hybrids of Type 1 and Type 2 curves. Both curves have a relatively constant slope to 0.8 μm with a decreasing slope to 1.3 μm, thus not exhibiting the concave character of the Type 1 curve or the convex character of the Type 2 curve. This Type 1 curve was described by Condit

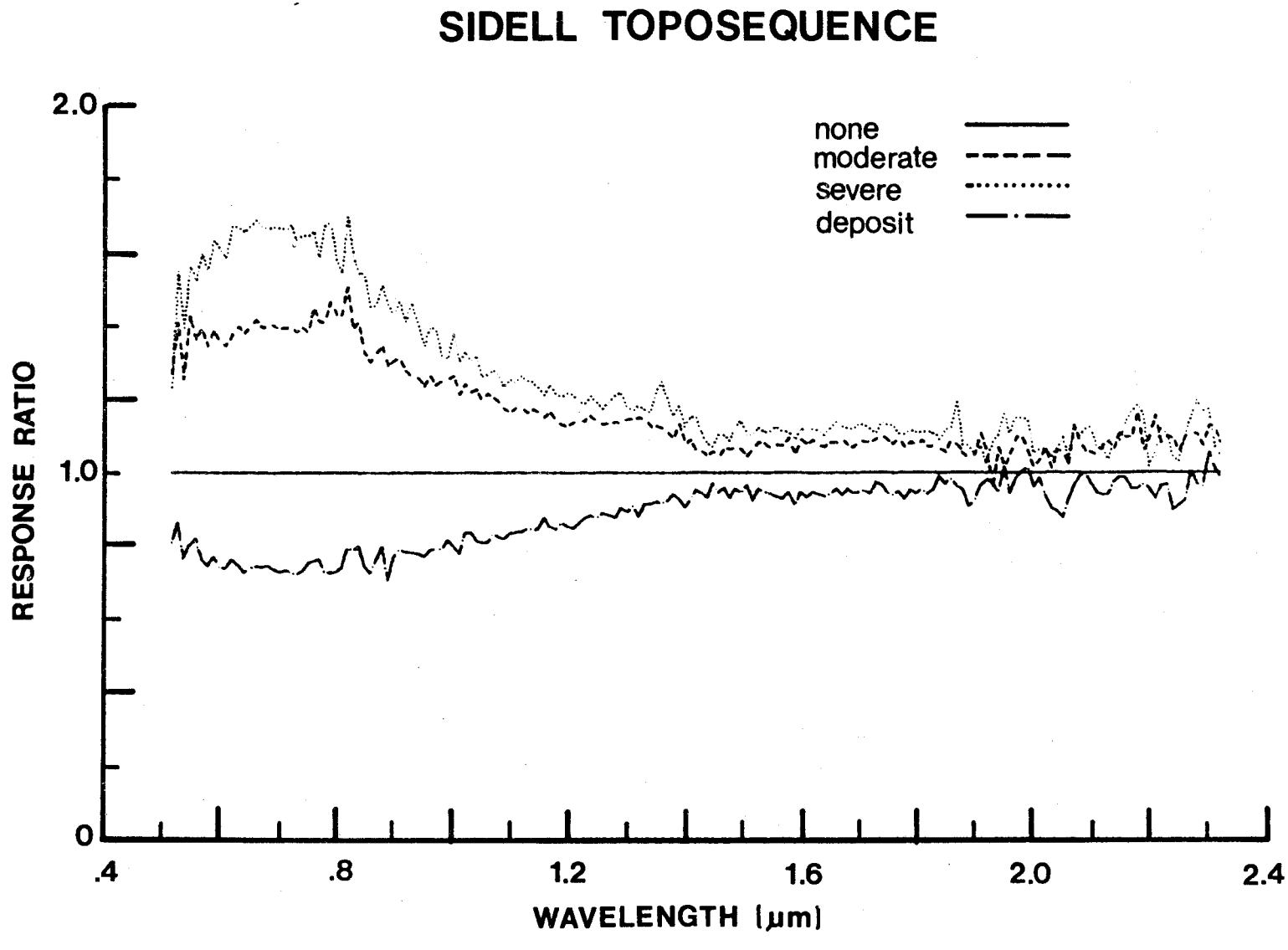

Figure 11. Response ratio curves of an eroded Sidell toposequence.

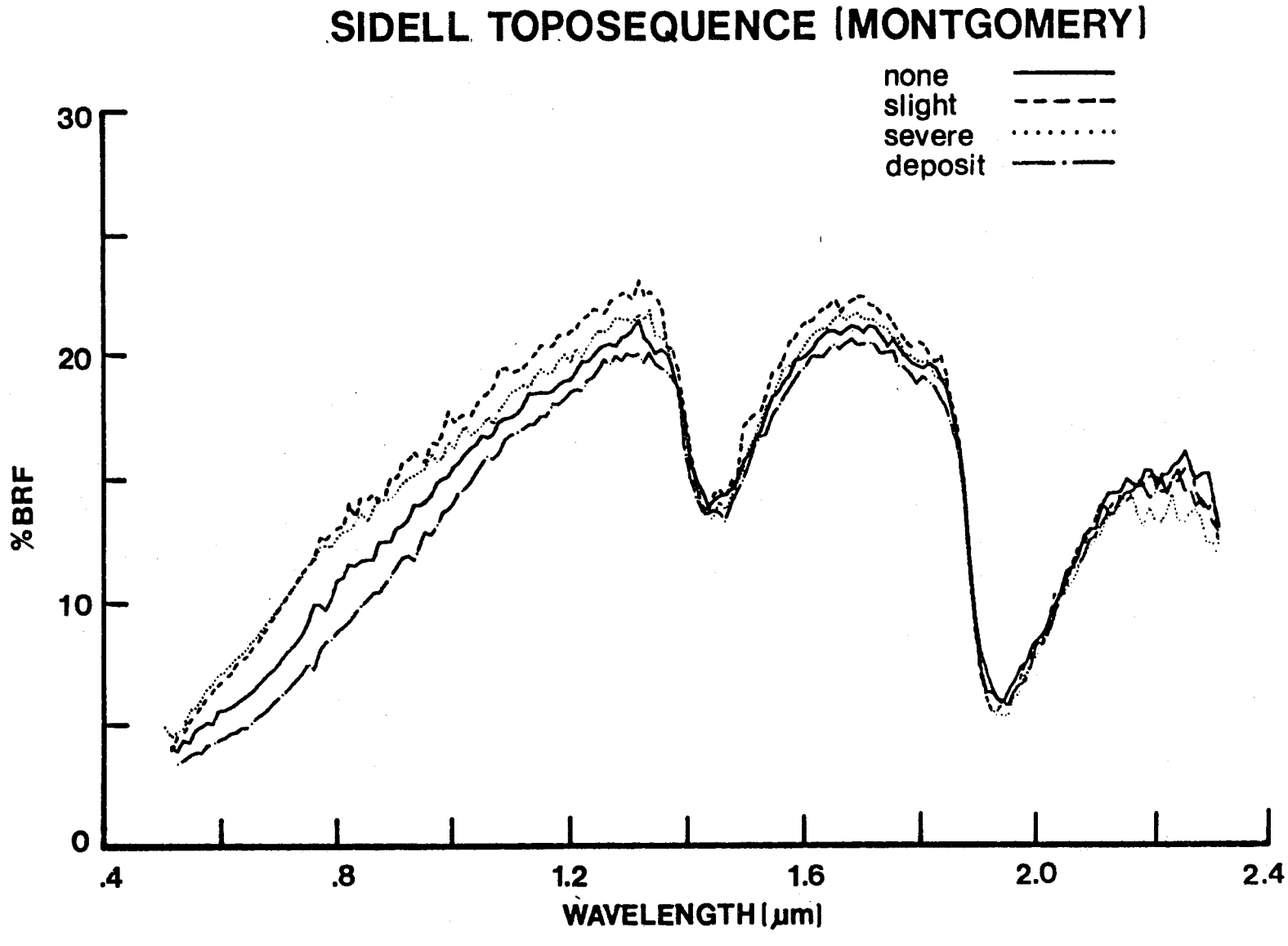

Figure 12. Reflectance curves of an eroded Sidell toposequence.

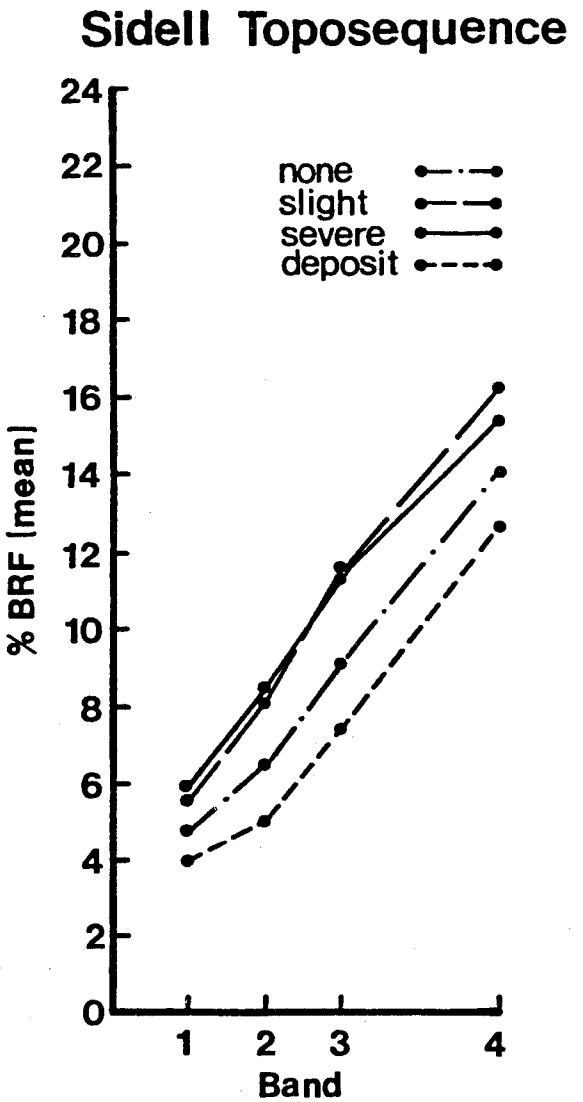

Figure 13. Simulated Landsat reflectance curves for an eroded Sidell toposequence.

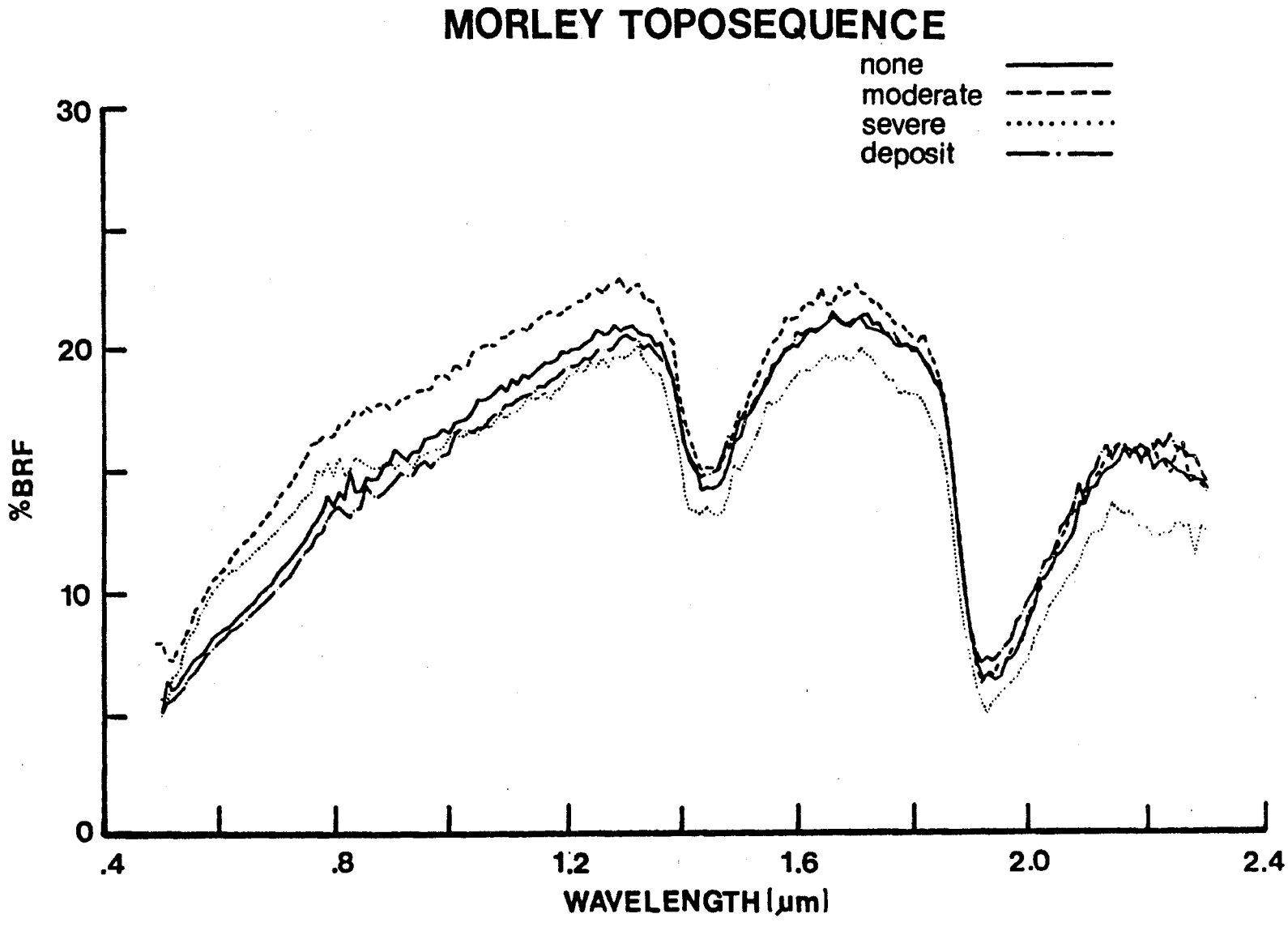

Figure 14. Reflectance curves of an eroded Morley toposequence.

(1970) as having the distinguishing feature of either increasing or nearly constant slope over any range of wavelengths from 0.32 to 1.00 μm. The curve of the moderately eroded soil decreases in the visible region to 0.67 μm, is somewhat constant to 0.77 μm and decreases in slope to 1.3 μm, resembling a Type 3 curve. The severely eroded soil curve has a more pronounced dip at 0.62 μm with zero slope from 0.77 to 0.95 μm. After 1.0 μm the severely eroded soil curve is almost inseparable from the depositional soil curve. The moderately eroded soil curve has the highest reflectance and the severe is next until it undercuts the none and depositional soil curves at 0.9 and 1.05 μm, respectively.

A standardized response ratio for the eroded Morley toposequence (Figure 15) demonstrates the similarity between the spectral curves of the uneroded soils. The ratio of the depositional soil has little curvature in general and almost parallels the standard curve up to 1.2 μm. The curvature of the moderately eroded soil ratio is concave to about 0.56 μm with nearly zero slope to 0.75 μm, then constant yet negative to 1.4 μm. The curvature of the severely eroded soil ratio indicates more distinct concavity than that of the moderately eroded soil to about 0.6 μm with a negative slope to 0.95 μm where the curve is almost inseparable from that of the depositional soil. The response ratio is highest for the curve of the moderately eroded soil and second for the severely eroded soil. Both eroded soil ratios are higher than the standard from 0.54 to 0.9 μm while the depositional soil ratio remains lower until 1.4 μm.

Reflectance curves of a Miami toposequence from Montgomery County, Indiana, are shown in Figure 16. The depositional soil curve is similar to the Type 1 curve with an increase in slope to 0.56 μm, a slight inflection from 0.58 μm, and a constant slope until 0.78 μm. The slight, moderate and severely eroded soil curves resemble the convex-shaped Type 3 curve. All three curves decrease in slope to about 0.8 μm, yet begin to demonstrate different degrees of slope to approximately 0.93 μm. The slightly eroded soil curve is somewhat constant, the moderately eroded soil curve is zero or decreases in slope and the severely eroded soil curve is relatively level. After 0.98 μm the slopes of the three curves decrease or are constant to 1.3 μm. The moderately eroded soil curve has the highest reflectivity; the severely and slightly eroded soil curves are similar until the 0.8 to 1.3 μm near infrared region where the severely eroded soil curve undercuts the slightly eroded soil curve. The depositional soil curve shows the least reflectance throughout the spectrum.

Figure 17 graphs the four simulated Landsat bands for the Miami toposequence. The depositional soil curve is almost constant in bands 1 to 3 and decreases slightly in band 4. The moderate, slight and severely eroded soil curves are similar to each other in bands 1 and 2 and are more separable in bands 3 and 4. The curves of the slight and moderately eroded soils are similar yet separable in bands 3 and 4 as they decrease in slope. The curve of the severely eroded soil undercuts the slightly eroded soil curve around band 3 with a more distinct decrease in slope. The moderately eroded soil curve is the most highly reflective throughout bands 1 to 4, the curve of the severely eroded soil is second until it becomes lower than the slightly

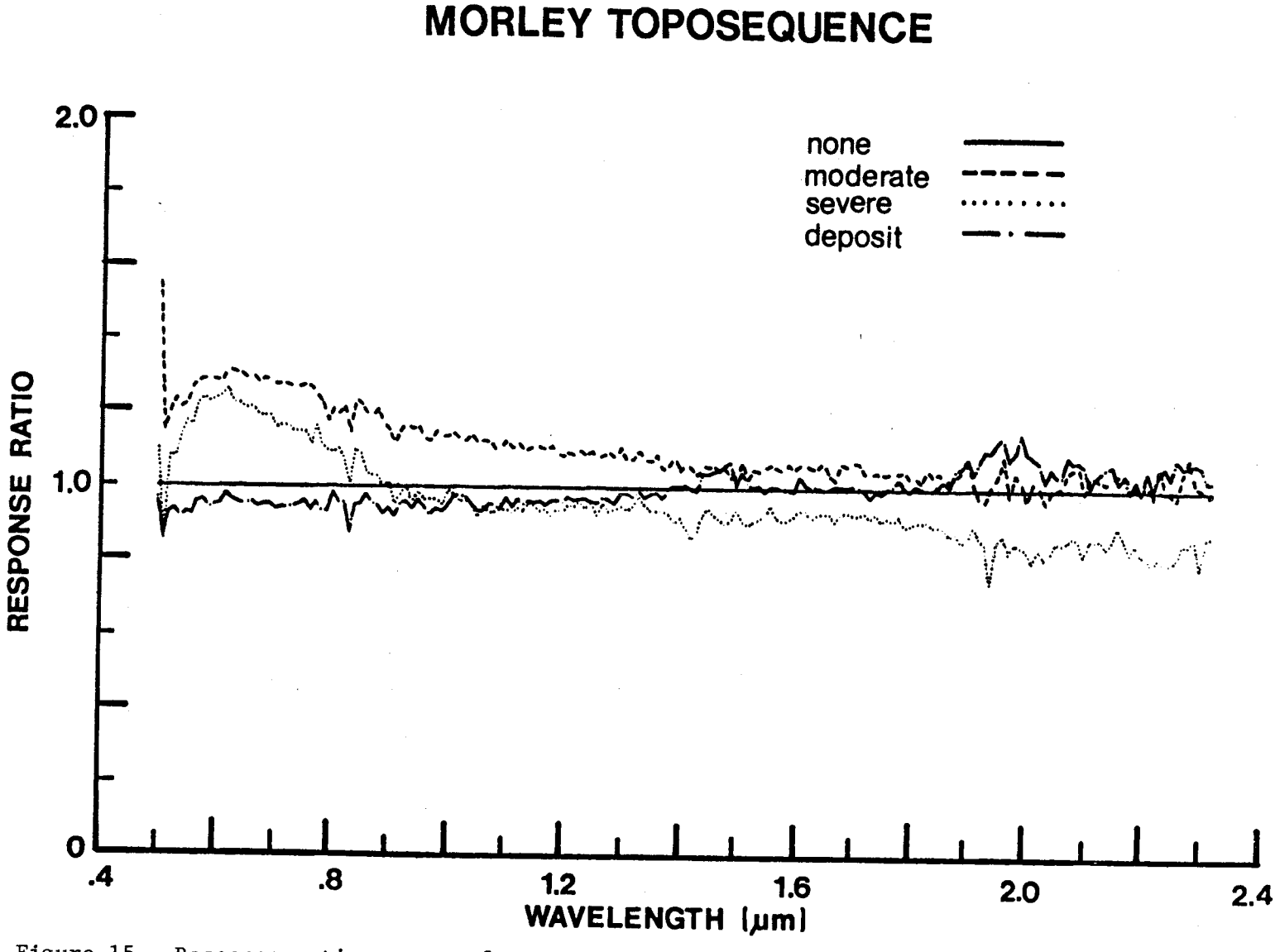

Figure 15. Response ratio curves of an eroded Morley toposequence.

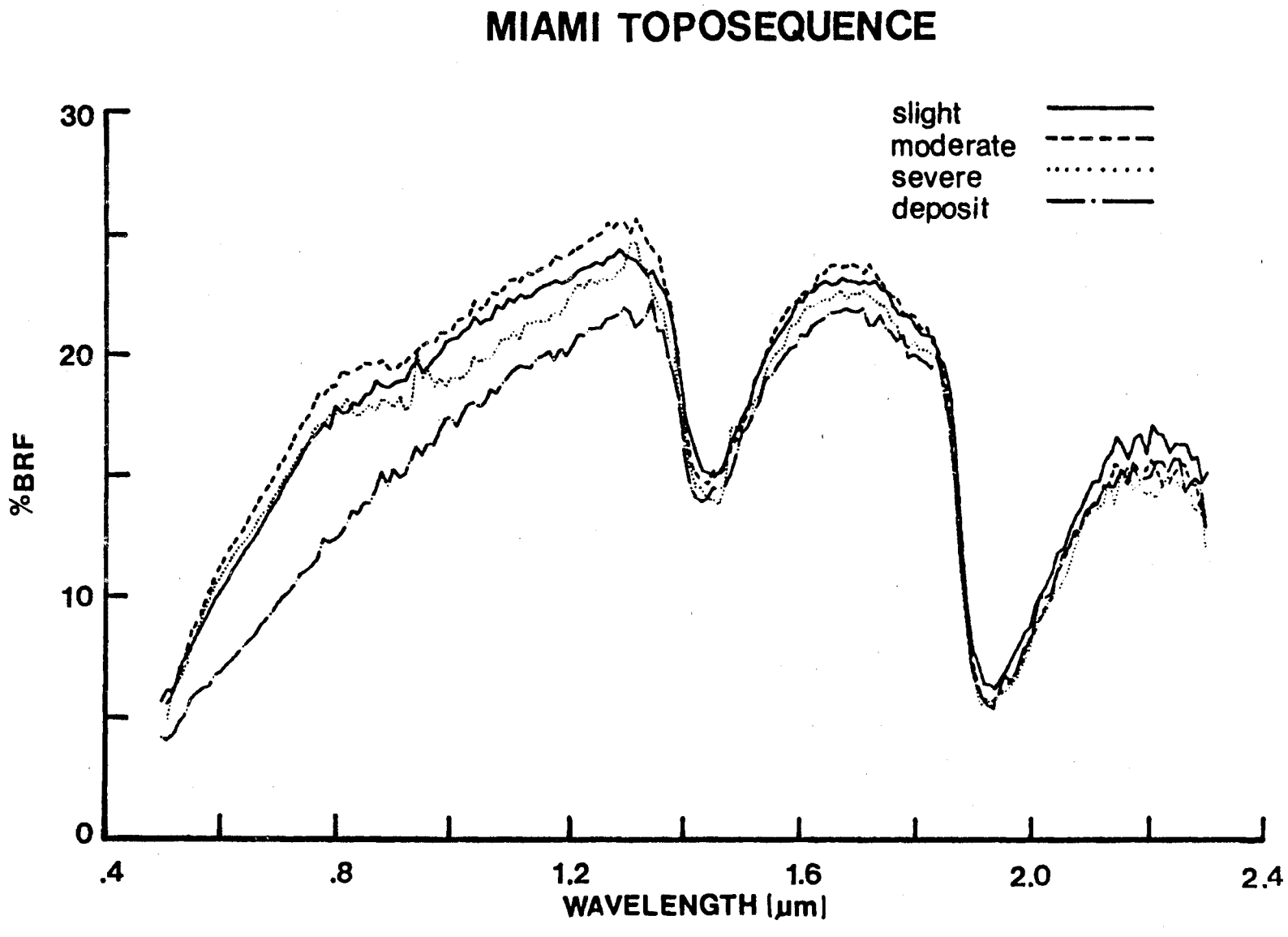

Figure 16. Reflectance curves of an eroded Miami toposequence.

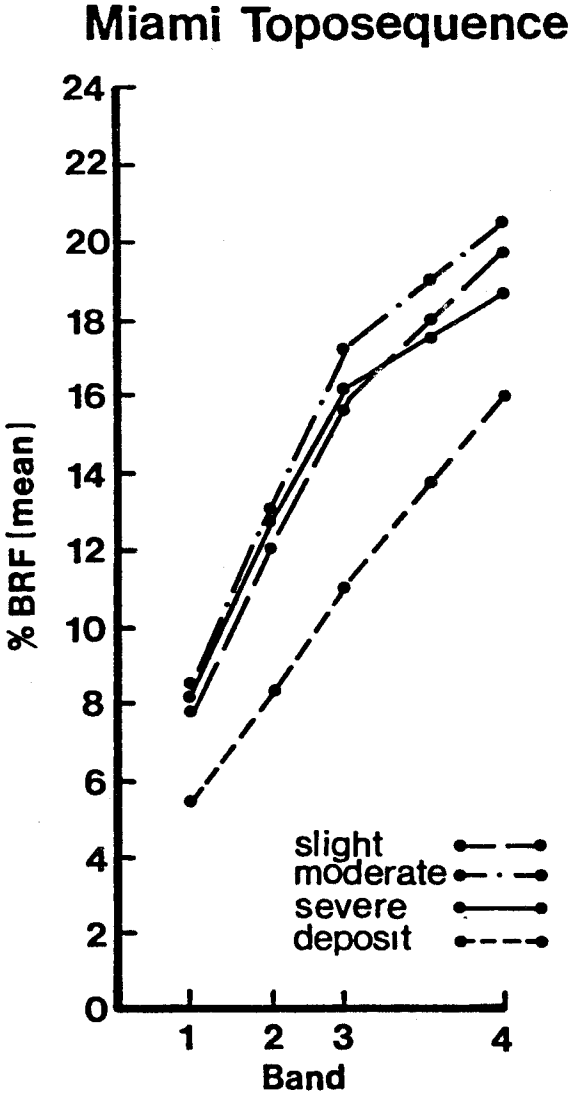

Figure 17. Simulated Landsat reflectance curves for an eroded Miami toposequence.

eroded soil curve around band 3. The depositional soil curve is clearly separable and is the least reflective of the spectral curves in this toposequence.

Figure 18 plots the reflectance curves of a Bedford toposequence from Orange County, Indiana. The non-eroded soil curve resembles the convex-shaped Type 2 curve that decreases in slope throughout the visible and near infrared spectral region. The slight and moderately eroded spectral curves are inseparable from 0.52 to 0.58 μm. The slightly eroded soil curve continues decreasing in slope until the slope becomes zero or negative from 0.78 to 0.9 μm then decreases to 1.3 μm. The moderately eroded soil curve decreases in slope to 0.77 μm, remains somewhat constant to 1.0 μm, then decreases to 1.3 μm. Both curve shapes resemble the Type 3 curve. The slightly eroded spectral curve of this toposequence has the highest reflectance from 0.6 to 1.1 μm, but at other wavelengths is almost inseparable from the moderately eroded spectral curve. The non-eroded curve has lower reflectance than both eroded curves.

Figure 19 measures the spectral reflectance of a Frederick toposequence from Lawrence County, Indiana. The spectral curves show little difference from each other until 0.6 μm where they separate into two distinct curves. The more reflective group of curves includes the none, moderate and severely eroded soils and the less reflective group of curves includes those of the very severely eroded and depositional soils. Only two curve shapes can be distinguished until 0.75 μm. Each curve shape can be separated from the others to 1.1 μm. From 0.75 to 0.95 μm the curves of the eroded and depositional soils have slightly decreasing or zero slope while the curve of the non-eroded soil is nearly constant. All of the curves decrease in slope from 0.95 to 1.3 μm. The curve of the non-eroded soil has the highest reflectance. At greater than 0.9 μm the curve of the severely eroded soil has the second highest reflectance, and the curve of the moderately eroded soil is third. The curves of the depositional and very severely eroded soils are most separable from 0.8 to 1.0 μm as the reflectance of the very severely eroded soil becomes lower than the reflectance of the depositional soil. All of the spectral curves resemble the convex-shaped Type 3 curve.

Figure 20 is an example of a graph of the Landsat bands plotted for the Frederick toposequence. All of the curves are convex-shaped with the spectral curve of the non-eroded soil having the highest reflectivity in all four Landsat bands. The curve of the moderately eroded soil shows the second highest reflectance measurements in bands 1 to 3 then decreases in slope to undercut the curve of the severely eroded soil. The spectral curves of the very severely eroded and depositional soils are lower in reflectance than the other curves with the curve of the depositional soil showing more reflectance than the very severely eroded soil curve in band 1. Bands 2 and 3 show slight differences in the two curves, but at band 4 the very severely eroded soil showed the lowest spectral reflectance of the Frederick toposequence.

The bidirectional response ratio of the eroded Frederick toposequence is plotted in Figure 21. At most of the wavelengths studied the response ratio of this toposequence is lower than the non-eroded soil standard. The curves

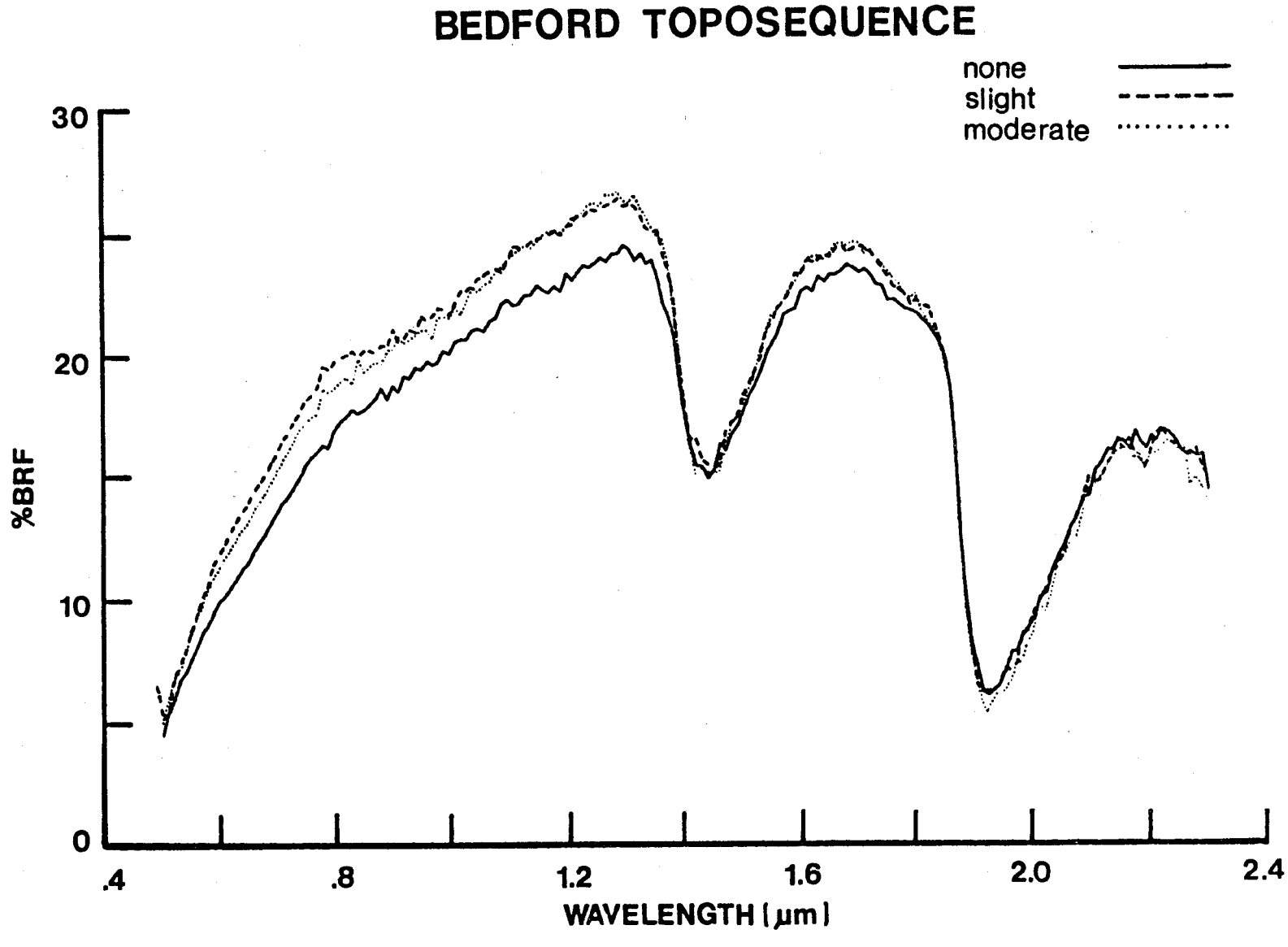

Figure 18. Reflectance curves of an eroded Bedford toposequence.

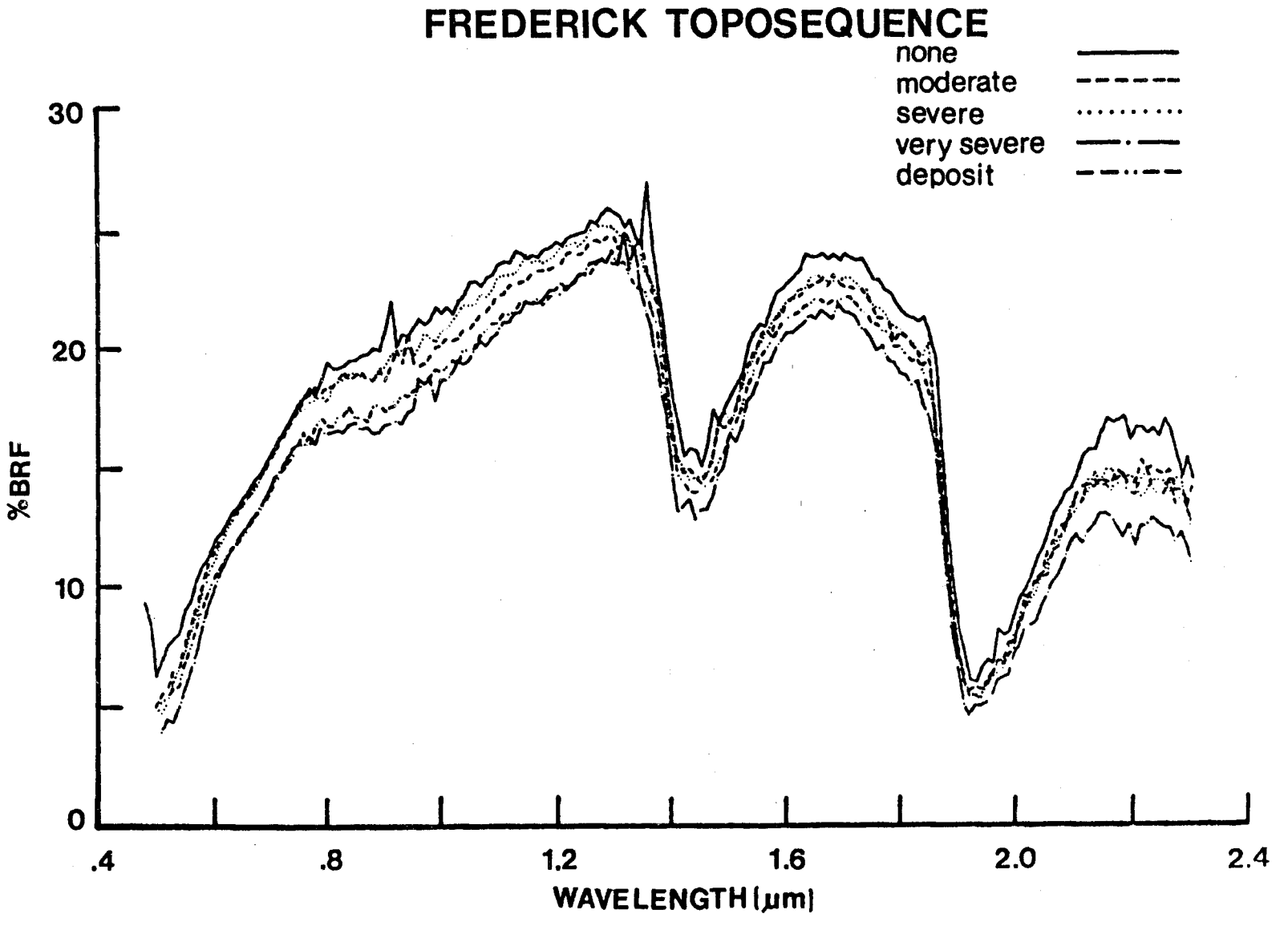

Figure 19. Reflectance curves of an eroded Frederick toposequence.

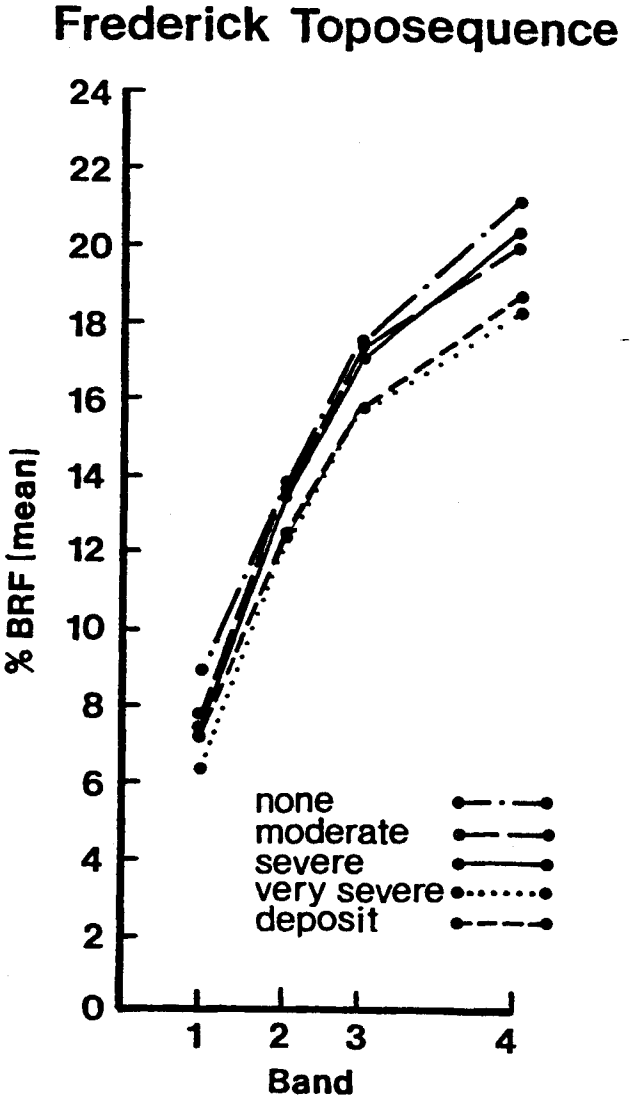

Figure 20. Simulated Landsat reflectance curves for an eroded Frederick toposequence.

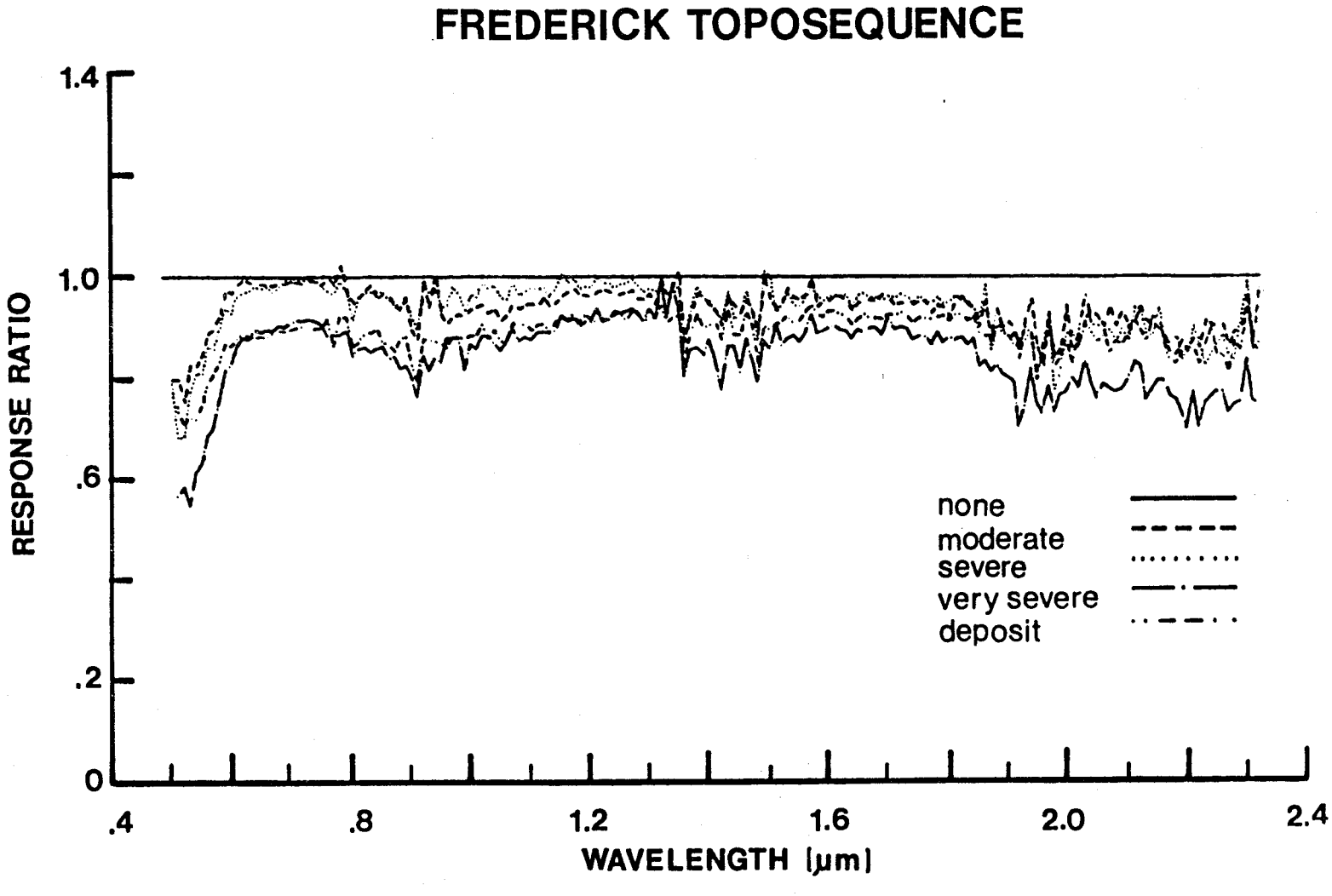

Figure 21. Response ratio curves of an eroded Frederick toposequence.

of the depositional and very severely eroded soils are most easily separated from 0.52 to 0.6 μm and beyond 0.6 to 1.3 μm the curves nearly coincide. From 0.52 to 0.6 μm the curve of the severely eroded soil has a lower response ratio than the curve of the depositional soil. There is little slope of either curve from 0.6 to 0.8 μm until the slope decreases into a distinct peak at 0.9 μm. The curvature of the moderate and severely eroded soil ratios are similar to about 0.9 μm. From 0.54 to 0.6 μm the slopes decrease and little curvature can be observed until the peak at 0.8 μm. The slope decreases negatively into a stronger peak at 0.9 μm and the two curves separate to 1.3 μm with the severely eroded soil having the higher response ratio.

Figure 22 shows the reflectance curves of the soils classified as none to slightly eroded from the Russell profile. The spectral curve of sample one is slightly concave-shaped and increases in slope until 0.8 μm, then decreases in slope. This is characteristic of a Type 1 curve although the degree of cancavity is subtle. The second sample shows a similar response to the third and fourth sample curves, all of which have decreasing slopes from 0.55 to 1.3 μm. The curves of the third and fourth samples nearly coincide and are more highly reflective than the curves of the first two samples. The first sample of this profile has the least reflective spectral curve. The spectral reflectance increases as depth increases in the first three samples. The first two curves resemble the Type 1 curve whereas the third and fourth curves are more like the convex-shaped Type 2 curve.

Five soil samples were classified as moderately eroded soils (Figure 23). Curves 5 and 6 resemble curves 3 and 4 (Figure 22), which have a general decrease in slope from 0.55 to 1.3 μm and resemble the Type 2 curve. The spectral curves of samples 7 to 9 are almost inseparable, yet higher in reflectance than samples 5 and 6. These curves resemble the Type 3 curve which decreases in slope to 0.8 μm, is relatively constant from 0.8 to 1.0 μm, and decreases in slope to 1.3 μm. Only two sets of curves are separable, the lower reflectance curve consisting of the curves of samples 5 and 6, and the higher reflectance curve consisting of the curves of samples 7, 8 and 9. From 0.8 to 1.3 μm, the most highly reflective curve is sample 8.

The last six samples of the Russell profile were classified as severely eroded soils (Figure 24). The spectral curves of the samples are almost inseparable except in isolated wavelengths around 0.8, 1.3 and 2.2 μm. The slope of this series of curves decreases to around 0.8 μm, levels off or becomes negative to 0.9 μm, increases to 1.0 μm and then decreases to 1.3 μm. This series of curves resembles the convex-shaped Type 3 curve.

Averages of the spectral reflectance data for the Russell soils classified as none to slight, moderate and severely eroded were calculated and graphs of the Landsat bands were plotted (Figure 25). All three of the curves are convex-shaped and the convexness appears to become stronger as the degree of erosion increases. The curve of the none to slightly eroded soils is the least reflective whereas the spectral curve of the severely eroded soils is more highly reflective in all four bands.

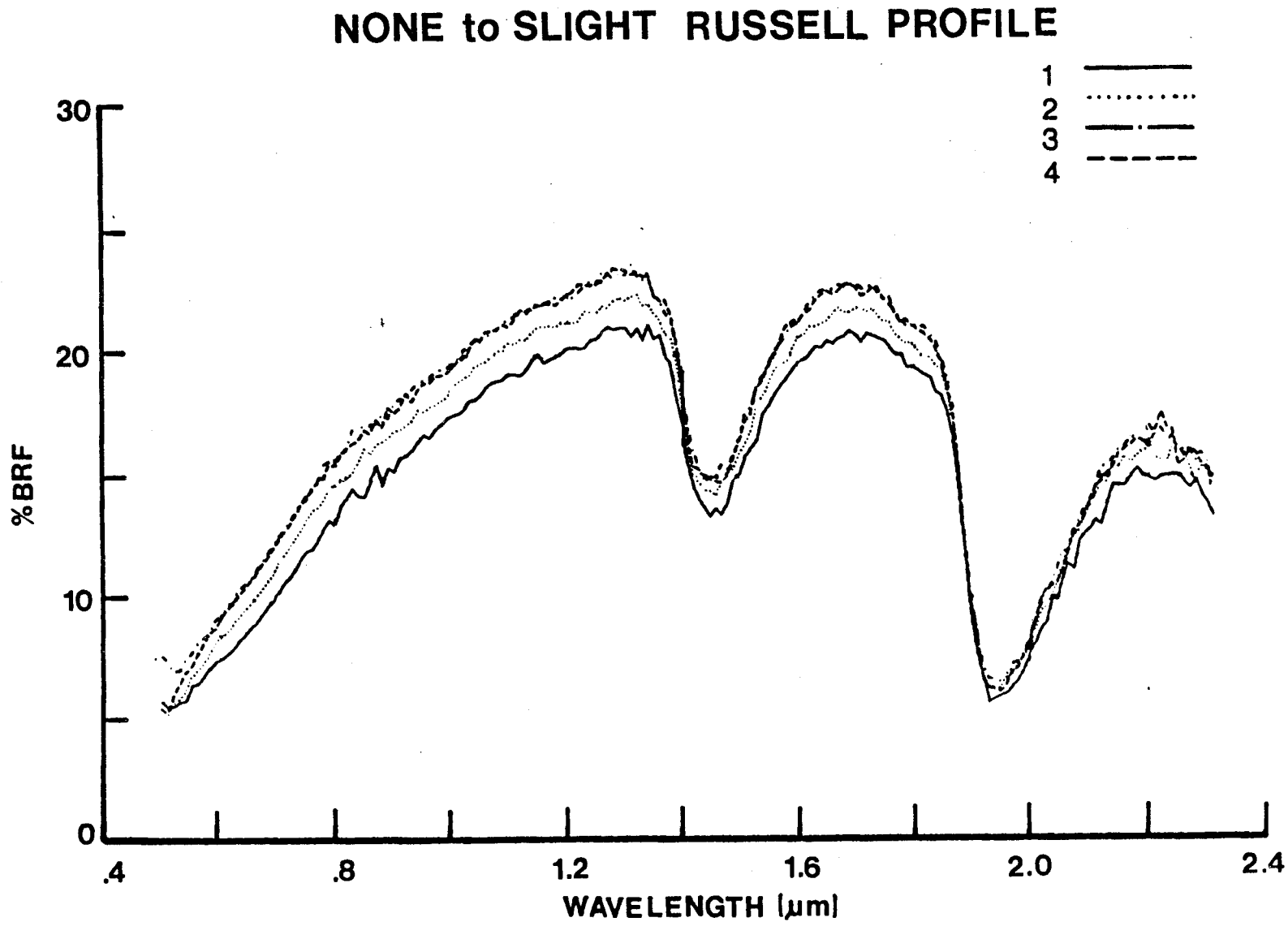

Figure 22. Reflectance curves of none to slightly eroded soils for the Russell profile.

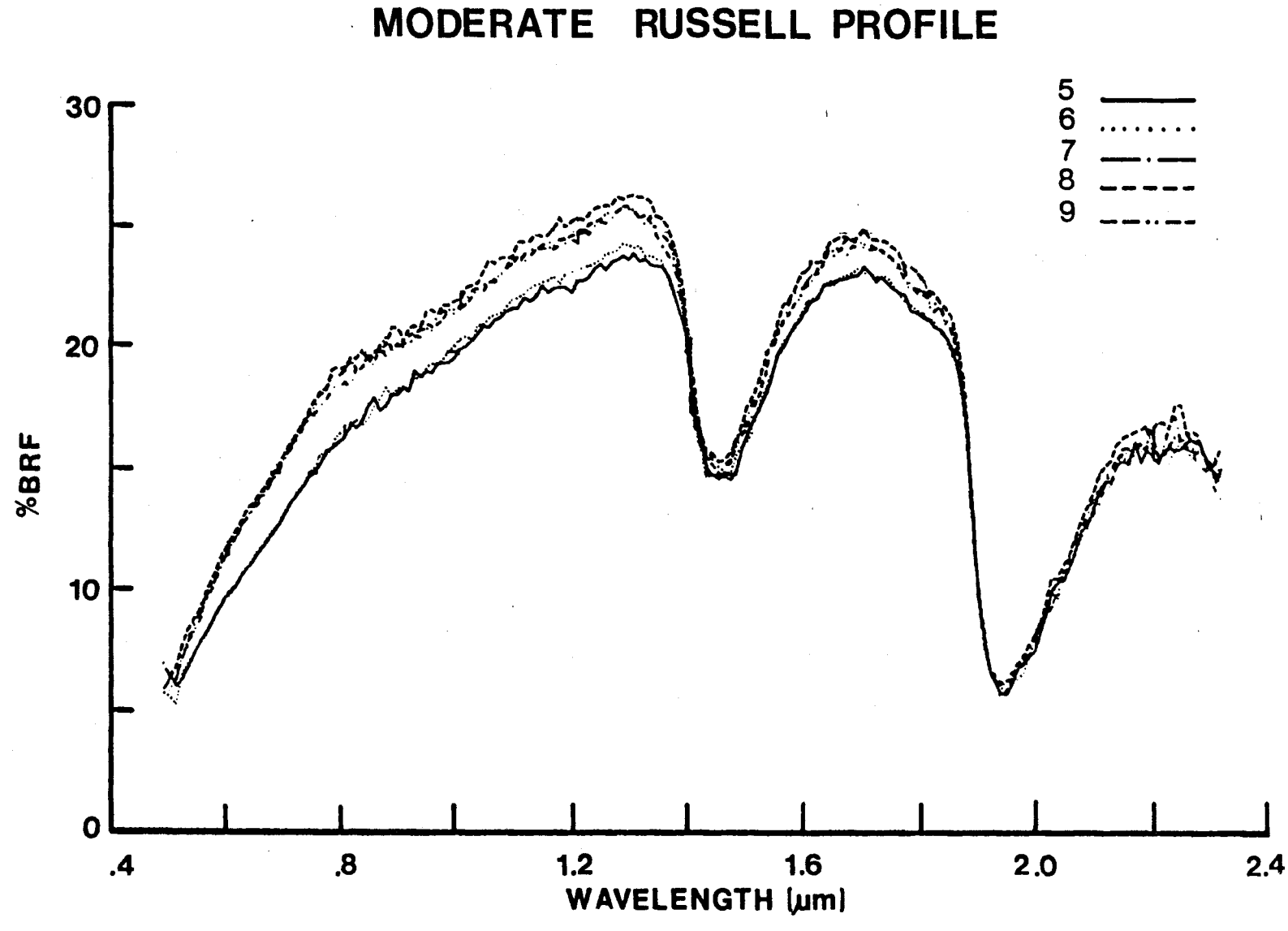

Figure 23. Reflectance curves of moderately eroded soils for the Russell profile.

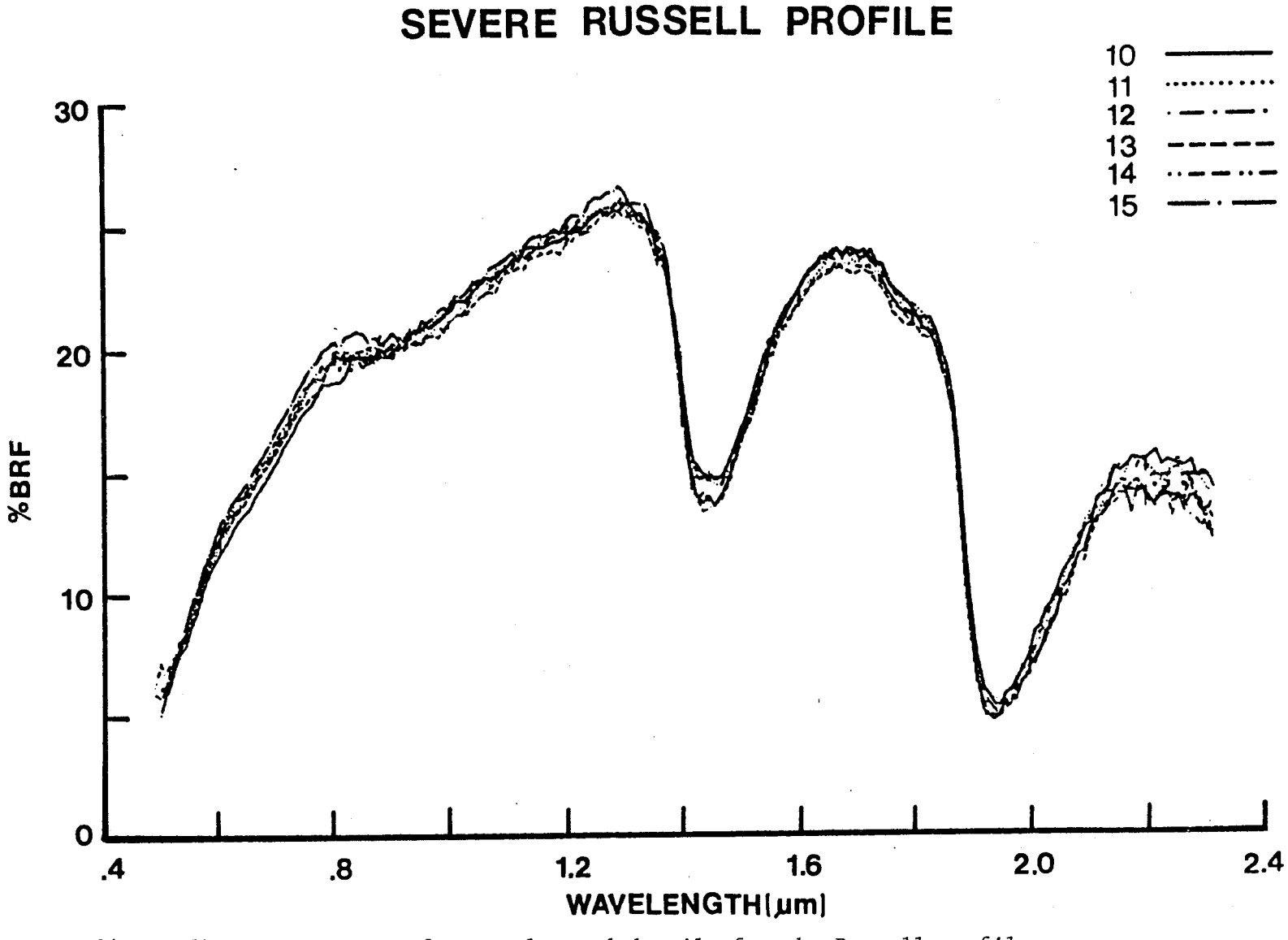

Figure 24. Reflectance curves of severely eroded soils for the Russell profile.

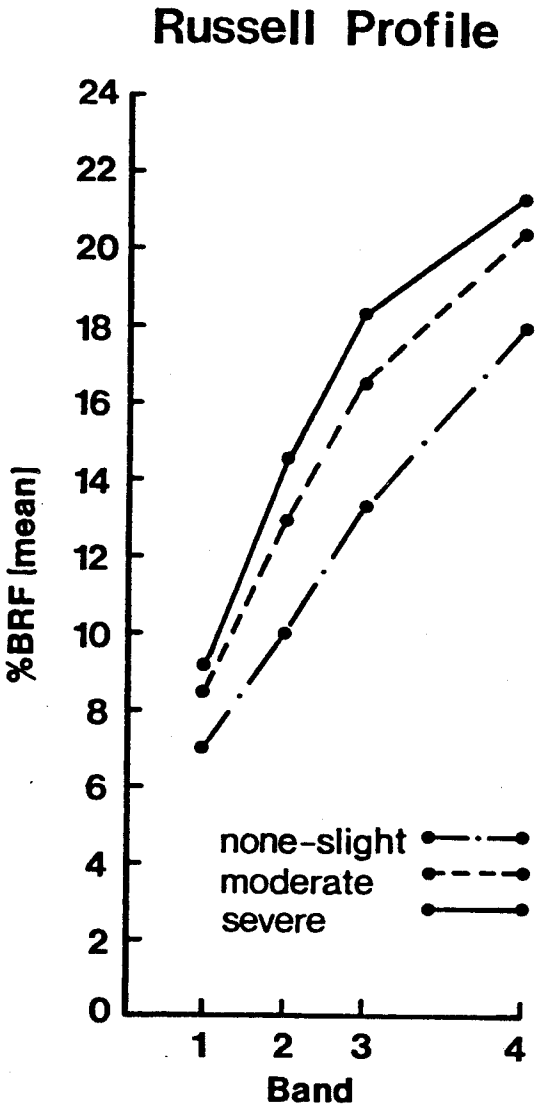

Figure 25. Simulated Landsat reflectance curves for the erosion classes of the Russell profile.

Relationship between Soil Parameters and Reflectance Curves

Organic matter tends to accumulate in surface soils due to the decomposition of plant and animal residues. High amounts of amorphous iron are associated with horizons having the most intense weathering and high pH-dependent charges such as humus, the dark-colored fraction of organic matter (McKeague and Day, 1966). The dark brown to black surface horizon of Mollisols may penetrate deep into the profile due to a slight decrease in organic matter from the Ap to A3 horizon followed by a more distinct decrease in organic matter in the B horizon. The leached A2 horizon of Alfisols is usually lighter in color than either the Ap or B horizons due to the translocation of humus, iron and clay whereas Ultisols are more difficult to classify by organic matter content and/or color because of intensive leaching and weathering of these soils.

The B2 horizon, the zone of maximum accumulation, tends to be higher in translocated clay and iron content. Increases in clay may increase the moisture content (Montgomery et al., 1976) and the cation exchange capacity of the soil due to the physical properties and negative charge of the clay particles. The iron oxide ratio is expected to increase with depth in the soil profile. This may be the result of higher properties of crystalline iron and/or lower proportions of amorphous iron associated with the depth of the soil horizon.

The spectral reflectance of soils with lower organic matter content tend to be influenced by the iron content (Baumgardner et al., 1970). This suggests that the effect of iron may be more pronounced in eroded soils. Increases in the iron content of eroded soils may be manifested in the iron absorption bands of the spectral reflectance curves.

The concave Type 1 curve shapes of the uneroded soils of the Sidell toposequences support the findings of Stoner and Baumgardner (1980) which classify these soils as having high organic matter contents characteristic of Mollisols. Throughout the entire spectrum scanned, the curve of the depositional soil has the lowest reflectance and the curve of the non-eroded soil is the next lowest. Other similarities between these uneroded soils are the dark-colored surface horizon and higher moisture content compared to the eroded soils in these toposequences. As would be expected, the position of these soils on the nearly level or depressional slope of the toposequence would allow more water to infiltrate and increase the accumulation of organic matter. The amount of amorphous iron associated with the organic matter in the uneroded and slightly eroded soils is equal to or higher than the amorphous iron found in the more eroded soils of these Mollisol toposequences (Figure 3 or 3a). The Type 1 curve as described by Condit (1970) includes the uneroded Alfisols and the first two samples of the Russell profile. The constant slope of these reflectance curves may be influenced by the organic matter content.

The convex-shaped Type 2 curve includes the spectral curves of the eroded soils of the Mollisol toposequences and the non-eroded soil of the Bedford (Ultisol) toposequence. In addition to the spectral curves of the third and

fourth slightly eroded soils of the Russell (Alfisol) profile, the first two moderately eroded soil samples were also labeled Type 2. The laboratory analysis of the eroded soils within the Mollisol toposequences indicate that these soils contain lower organic matter and moisture contents than the uneroded soils in the respective toposequences. This is consistent with respect to their more sloping topographic position and their respective location within the soil catena which could accelerate water run-off and loss of surface soil, including organic matter and amorphous iron oxide. This decrease in organic matter, amorphous iron oxide and moisture content may cause an increase in the spectral reflectance of these eroded soils (Obukhov and Orlov, 1964; Stoner and Baumgardner, 1980; Bowers and Hanks, 1965).

Some soils from the Alfisol soil order and certain Ultisols can be seen to exhibit this Type 2 curve shape (Stoner and Baumgardner, 1980). It was observed that these Alfisols have a darker color, more organic matter and more or at least equal amounts of amorphous iron oxide compared to the eroded soils in their toposequences. The same concept of uneroded versus eroded soils appears to be consistent between the Alfisol and Mollisol toposequences with respect to color, organic matter and amorphous iron oxide. At the same time little relationship was observed with the organic matter and the non-eroded Bedford sample yet this soil was higher in amorphous iron and lower in total iron oxide and the iron oxide ratio than the eroded soils in this toposequence. Intensive leaching and weathering of Ultisols may place greater emphasis on the effect of iron oxide compounds on spectral reflectance whereas the organic matter may play the more important role in spectral reflectance of Mollisols.

The spectral reflectance of the Russell profile appears to increase with sample depth. This may be a function of the loss of organic matter, the gain of total iron oxide or a combination of these and other soil parameters including color and moisture.

Measurements of the Russell profile indicate that each of the Type 1 and Type 2 samples contain at least 60% A horizon with greater than 1% organic matter. These samples averaged lower values in each iron oxide category than samples deeper in the profile. It is reasonable to expect lower amounts of total iron and iron oxide ratio in the upper section of the profile while the nearly equal amounts of amorphous iron oxide may be affected by the lower organic matter content of this soil.

The reflectance curves of the uneroded soils of the Frederick (Ultisol) toposequence, the eroded soils of the Alfisol and Ultisol toposequences and the lower nine Russell profile samples (moderate and severly eroded) were identified as Type 3 curves. This convex-shaped curve differs from the Type 2 curve by exhibiting a leveling off of the slope from near 0.75 to 0.9 μm. Stoner and Baumgardner (1980) found that moderately high free iron oxide contents are observed in most Type 3 curves. The results of the laboratory analysis indicate that the eroded soils listed above contain nearly equal, if not higher, amounts of total iron oxide content in comparison to the uneroded soils in their respective toposequences. The Frederick toposequence has the highest overall average of total iron oxide and iron oxide ratio. Although

the relationship between amorphous iron oxide content and degree of erosion and/or spectral reflectance was not strong, the iron oxide ratio was highly correlated with the degree of erosion. The variability found in the Frederick data may be a function of the iron oxide ratio plus the masking effect of the organic matter on the spectral properties of various forms of iron oxide. The same argument can be used with these Russell samples where each sample contains at least 50% B horizon and less than or equal to 1% organic matter. These samples also demonstrate increases of total iron oxide and iron oxide ratio with depth which may influence the spectral curves. This suggests that more attention be given to the iron oxide ratio and the organic matter content rather than concentrating primarily on total iron oxide.

As the spectral curves of the eroded soils level off from about 0.75 to 0.9 μm, the curves of the uneroded soils continue to increase in reflectance. This situation could account for the undercutting of the spectral curves of the severely eroded soils in the near infrared region, i.e., the Sidell (Mont.) and Alfisol toposequences.

The greatest separability in most of the spectral reflectance curves is from about 0.55 to 1.3 μm. At wavelengths greater than 1.3 μm, the spectral curves are strongly influenced by the clay and water absorption bands at 1.4 and 1.9 μm. Based upon spectral data from early research, the present Landsat bands were designed to measure the reflectance from 0.5 to 1.1 μm.

Several examples of simulated Landsat graphs were produced to determine the practicality of using actual Landsat MSS data to delineate eroded soils under natural conditions. The graphs verify the general trend of the slope of the spectral curves. Three curve types are represented and are quite separable, i.e., 1) the uneroded Sidell (Mollisol) and depositional Miami (Alfisol), 2) the eroded Sidell and 3) the eroded Miami and all of the Frederick (Ultisol) toposequence.

Each of these Landsat graphs (Figures 13, 17 and 20) demonstrates the curve of an eroded soil undercutting another spectral curve between band 3 and 4 as also seen in the laboratory data (the eroded soil curve has a less positive slope than the other soil curve). At this point, the slope of that curve decreases more acutely than elsewhere in the spectrum. Inferences from the chemical analysis of these toposequences suggest that a combined effect of the organic matter, total and amorphous iron oxide contents may strongly influence the slope of the curve.

The graphs of the standardized bidirectional response ratio emphasize the concave and/or convex shapes of the spectral curves and the wavelength regions of best separability between these curves in relation to the non-eroded standard curve. These examples verify that the response ratio of the depositional soil is lower than the non-eroded standard. In the Mollisol toposequence, the curvature of the depositional soil is more concave than the standard whereas the Alfisol and Ultisol toposequences indicate a more parallel relationship between the uneroded soils. The eroded soils tend to be separable from the depositional soils; as the convex curvature increases, it appears that the degree of erosion increases. By measuring the change in

the response ratio from 0.53 to 0.6 μm in the Frederick toposequence, a greater change in the response ratio tends to indicate a greater degree of erosion.

The best separability among these curves is from 0.53 to about 0.9 μm although the Mollisol shows slight changes in slope to 1.4 μm. Beyond 1.4 μm there is little to interpret in these curves as most of the slopes are relatively parallel to the standard and difficult to separate from each other.

CONCLUSIONS AND SUMMARY

The soil parameters that appeared to affect the spectral reflectance the most were organic matter and iron oxide content and the iron oxide ratio. Higher amounts of organic matter may have the ability to mask the higher iron oxide content of the spectral reflectance curves of the eroded Mollisols whereas the spectral curves of eroded Alfisols and Ultisols showed more prominent iron absorption bands. The effects of erosion may be detected at about 0.8 μm; higher iron oxide contents may tend to broaden the wavelength range over a 0.1 μm range. Although the amorphous iron oxide content showed little correlation with respect to erosion or spectral reflectance, the iron oxide ratio was the one parameter that was most consistent among the six toposequences and the Russell profile. The highest iron oxide ratio occurred in the severely eroded soils. As the degree of erosion decreased, the iron oxide ratio decreased. This suggests that less eroded soils may contain lower crystalline iron oxide and/or higher amorphous iron oxide and more eroded soils may increase in crystalline iron oxide and/or decrease in amorphous iron oxide.

Knowledge of the soil order and relative position within a catena would greatly aid in the identification of eroded soils by spectral reflectance measurements, especially if significance is to be placed on the specific curve types and slopes between 0.75 and 0.9 μm (Landsat bands 3 and 4). The eroded Mollisol and Ultisol toposequences may be more difficult to identify without field data or comparisons of these soils to the uneroded soils within the particular toposequence. Interference from organic matter and/or total iron content may mask the erosion class. The eroded soils of the Alfisol toposequences were identified by their Type 3 curve shape, but the spectral reflectance of the Russell (Alfisol) profile suggested that differences between degrees of erosion within the soils classified as moderately eroded may not be as easily separated. As demonstrated in the Alfisol toposequences, the none to slightly eroded soils were separable from the severely eroded soils by their curve shapes.

The spectral curves as plotted by the Landsat bands illustrated that the eroded soils were separable from the uneroded soils, assuming prior knowledge of the soil order and relative position within a catena. The most important difference in the spectral reflectance appeared around 0.8 μm or band 3 in

the Landsat graph. Although the detailed leveling off of the slope of the curve was not as obvious as in the continuous scan of the spectrum, a distinct decrease in slope and even the undercutting of several of the curves could be evidenced from band 3 to 4.

The majority of information utilized for the spectral analysis of these soils was in the visible and near infrared region. This area was covered by the Landsat bands and could provide sufficient data to aid in the detection and identification of eroded soils.

LIST OF REFERENCES

Al-Abbas, A. H., P. H. Swain and M. F. Baumgardner. 1972. Relating organic matter and clay content to the multispectral radiance of soils. Soil Sci. 114(6):477-485.

Angstrom, A. 1925. The albedo of various surfaces of ground. Geografiska Ann. 7:323.

Baumgardner, M. F., S. J. Kristof, C. J. Johannsen and A. Zachary. 1970. Effects of organic matter on the multispectral properties of soils. Proc. of the Indiana Academy of Science 79:413-422.

Beck, R. H., B.F. Robinson, W. W. McFee and J. B. Peterson. 1976. Spectral characteristics of soils related to the interaction of soil moisture, organic carbon and clay content. LARS Information Note 081176. Laboratory for Applications of Remote Sensing, Purdue University, West Lafayette, IN.

Bowers, S. A. and R. J. Hanks. 1965. Reflection of radiant energy from soils. Soil Science 100(2):130-138.

Bushnell, T. M. 1951. Use of aerial photography for Indiana land studies. Photogrammetric Engineering 17:725-738.

Carroll, D. M. 1973a. Remote sensing techniques and their application to soil science. Part I. The photographic sensors. Soils Fert. 36:259-266.

Cihlar, J. and R. Protz. 1973. Surface characteristics of mapping units related to aerial imaging of soil. Can. J. of Soil Science 53:249-257.

Cipra, J. E., M. F. Baumgardner, E. R. Stoner, R. B. MacDonald. 1971. Measuring radiance characteristics of soil with a field spectroradiometer. Soil Science Soc. of Amer. Proc. 35:1014-1017.

Condit, H. R. 1970. The spectral reflectance of American soils. Photogrammetric Engineering 36:955-966.

DeWitt, D. P. and B. F. Robinson. 1974. Description and evaluation of a bidirectional reflectance factor reflectometer. LARS Information Note 091576. Laboratory for Applications of Remote Sensing, Purdue University, West Lafayette, IN.

FAO. 1978. Methodology for assessing soil degradation. FAO-UNDP.

FAO. 1979. A provisional methodology for soil degradation assessment. FAO-UNDP. Rome, Italy.

Fink, D J. 1980. Earth observation - issues and perspectives. American Institute of Aeronautics and Astronautics 16th Annual Meeting and Technical Display. Baltimore, MD.

Franzmeier, D. P., G. C. Steinhardt, J. R. Crum and L. D. Norton. 1977. Soil characterization in Indiana. I. Field and laboratory procedures. Research Bulletin #943. Purdue University, West Lafayette, IN.

Gausman, H. W., A. H. Gerbermann, C. L. Wiegand, R. W. Leamer, R. R. Rodriguez and J. R. Noriega. 1975. Reflectance differences between crop residues and bare soils. Soil Sci. Soc. Am. Proc. 39:752-755.

Gerbermann, A. H. and D. D. Neher. 1979. Reflectance of varying mixtures of a clay soil and sand. Photogrammetric Engineering and Remote Sensing 45(8):1145-1151.

Guruswamy, V., S. J. Kristof and M. F. Baumgardner. 1980. A case study of soil erosion detection by digital analysis of the remotely sensed multispectral Landsat scanner data of a semi-arid land in southern India. Machine Processng of Remotely Sensed Data Symp., Purdue University, West Lafayette, IN. pp. 266-271.

Hinzel, E. J., R. A. Weismiller, and D. P. Franzmeier. 1979. Correlation of spectral classes derived from Landsat MSS data to soil series and soil conditions for Jasper County, Indiana. LARS Technical Report 080979. Laboratory for Applications of Remote Sensing, Purdue University, West Lafayette, IN.

Hudson, N. 1971. Soil Conservation. Cornell Univ. Press. p. 25.

Hunt, R. M. and J. W. Salisbury. 1970. Visible and near-infrared spectra of minerals and rocks. I. Silicate minerals. Modern Geology 1:283-300.

Hunt, G. R., J. W. Salisbury and C. J. Lenhoff. 1971b. Visible and near-infrared spectra of minerals and rocks. III. Oxides and hydroxides. Modern Geology 2:195-205.

Jackson, M. L. 1969. Soil Chemical Analysis. Advanced Course. 2nd edition, 8th printing, 1973. Published by the author, Dept. of Soil Sci., Univ. of Wisconsin, Madison, WI.

Jamison, V. C. and I. F. Reed. 1949. Durable asbestos tension table. Soil Science 67:311-318.

Johannsen, C. J. and M. F. Baumgardner. 1968. Remote sensing for planning resource conservation. Proc. of the 93rd Annual Meeting of the Soil Conservation Society of America. Athens, Georgia. pp. 149-255.

Kaminsky, S. A., R. A. Weismiller and B. O. Blair. 1979. An investigation of analysis techniques of Landsat MSS data designed to aid the soil survey. LARS Technical Report 080879. Laboratory for Applications of Remote Sensing, Purdue University, West Lafayette, IN.

Karmanov, I. I. 1970. Study of soils from the spectral composition of reflected radiation. Soviet Soil Sci. 4:226-238.

Karmanov, I. I. and V. A. Rozhkov. 1972. Experimental determination of quantitative relationships between the color characteristics of soils and soil constituents. Soviet Soil Sci. 4:666-677.

Kimberlin, L. W. 1976. Conservation treatment of erodible cropland: status and needs. in Soil Erosion: Prediction and Control. Proc. Conf. on Soil Erosion. West Lafayette, IN. pp.339-346.

Kirschner, F. R. 1979. Personal communication.

Kirschner, F. R., S. A. Kaminsky, R. A. Weismiller, H. R. Sinclair and E. J. Hinzel. 1978. Map unit composition assessment using drainage classes defined by Landsat data. Soil Sci. Soc. Am. J. 42:768-771.

Kohnke, Helmut. 1968. Soil Physics. McGraw-Hill Book Company, New York. pp. 96-97.

Kohnke, H. and A. R. Bertrand. 1959. Soil Conservation. McGraw-Hill Book Company, New York. pp. 1-26.

Krishnan, P., J. D. Alexander, B. J. Butler and J. W. Hummel. 1980. Reflectance technique for predicting soil organic matter. Soil Sci. Soc. Am. J. 44:1282-1285.

Kristof, S. J. 1971. Preliminary multispectral studies of soils. J. Soil Water Conserv. 26(1):15-18.

Kristof, S. J., M. F. Baumgardner and C. J. Johannsen. 1973. Spectral mapping of soil organic matter. LARS Information Note 030773. Laboratory for Applications of Remote Sensing, Purdue University, West Lafayette, IN.

Kristof, S. J., M. F. Baumgardner, R. A. Weismiller and S. M. Davis. 1980. Application of multispectral reflectance studies of soils: Pre-Landsat. 1980 Machine Processing of Remotely Sensed Data Symp. Purdue University, West Lafayette, IN.

Kristof, S. J., M. F. Baumgardner, A. L. Zachary and E. R. Stoner. 1977. Comparing soil boundaries delineated by digital analysis of multispectral scanner data from high and low spatial resolution systems. LARS Information Note 082477. Laboratory for Applications of Remote Sensing, Purdue University, West Lafayette, IN.

Kristof, S. J. and A. L. Zachary. 1971. Mapping soil features from multispectral scanner data. Photogrammetric Engineering 40(12):1427-1434.

Leamer, R. W. and B. Shaw. 1946. A simple apparatus for measuring noncapillary porosity on an extensive scale. J. Am. Soc. Agronomy 33:1103-1108.

Lowdermilk, W. C. 1953. Conquest on the land through seven thousand years. Agric. Info. Bull. 99, U. S. Dept. Agriculture.

Manual of Remote Sensing. 1975. American Society of Photogrammetry. Falls Church, Virginia.

Matthews, H. L., R. L. Cunningham, J. E. Cipra and T. R. West. 1973a. Application of multispectral remote sensing to soil survey research in southeastern Pennsylvania. Soil Sci. Soc. Am. Proc. 37:88-93.

Matthews, H. L., R. L. Cunningham and G. W. Petersen. 1973b. Spectral reflectance of selected Pennsylvania soils. Soil Sci. Soc. Am. Proc. 37:421-424.

McKeague, J. A., J. E. Brydon and N. M. Miles. 1971. Differentiation of forms of extractable iron and aluminum in soils. Soil Sci. Soc. Am. Proc. 35:33-38.

McKeague, J. A. and J. H. Day. 1966. Dithionite- and oxalate-extractable Fe and Al as aids in differentiating various classes of soils. Can. J. Soil Sci. 46:13-22.

Miller, D. M. 1981. The effect of simulated short-term weathering on the distribution of oxalate-soluble iron and aluminum in a till and a loess. M.S. Thesis. Purdue University. West Lafayette, IN.

Montgomery, O. L. and M. F. Baumgardner. 1974. The effects of the physical and chemical properties of soil on the spectral reflectance of soils. LARS Technical Report 112674. Laboratory for Applications of Remote Sensing, Purdue University, West Lafayette, IN.

Montgomery, O. L., M. F. Baumgardner and R. A. Weismiller. 1976. An investigation of the relationship between spectral reflectance and the chemical, physical and genetic characteristics of soils. LARS Information Note 082776. Laboratory for Applications of Remote Sensing, Purdue University, West Lafayette, IN.

Obukhov, A. I. and D. S. Orlov. 1964. Spectral reflectivity of major soil groups and the possibility of using diffuse reflection in soil investigation. Soviet Soil Sci. 2:174-184.

Orlov, D. S. 1966. Quantitative patterns of light reflection by soils I. Influence of particle (aggregate) size on reflectivity. Soviet Soil Sci. 13:1495-1498.

Planet, W. G. 1970. Some comments on reflectance measurements of wet soils. Remote Sensing Environ. 1:127-129.

Raad, A. T., R. Protz and R. L. Thomas. 1969. Determination of Na-dithionite and NH -oxalate extractable Fe, Al, and Mn in soils by atomic absorption spectroscopy. Can. J. Soil Sci. 49:89-94.

Robinson, A. R. and L. D. Meyer. 1976. The Agricultural Research Service national research program on soil erosion by water. in Soil Erosion: Prediction and Control. Proc. Conf. on Soil Erosion. West Lafayette, IN. pp. 90-96.

Schwertmann, U. 1964. The differentiation of iron oxide in soils by a photochemical extraction with acid ammonium oxalate. Z. Pflanzenernahr. Dung. Bodenkunde 105:194-201.

Schwertmann, U. and W. R. Fischer. 1973. Natural "amorphous" ferric hydroxide. Geoderma Intl. J. Soil Sci. 10:237-247.

Seubert, C. E., M. F. Baumgardner, R. A. Weismiller and F. R. Kirschner. 1979. Mapping and estimating areal extent of severely eroded soils of selected sites in northern Indiana. 1979 Machine Processing of Remotely Sensed Data Symp. Purdue University, West Lafayette, IN.

Silva, L. F. 1978. Radiation and Instrumentation in Remote Sensing. Remote Sensing: The Quantitative Approach. McGraw-Hill Book Company, New York. pp. 21-135.

Silva, L. F., R. M. Hoffer and J. E. Cipra. 1971. Extended wavelength field spectroradiometry. pp. 1509-1518. International Symp. on Remote Sensing of Environ. Proc. 7th Inst. of Science and Technology. Univ. of Michigan, Ann Arbor, MI.

Soil Erosion: Prediction and Control. 1976. Proc. Conf. on soil erosion. Purdue University, West Lafayette, IN. Soil Conservation Society of America. Special publication #21.

Stoner, E. R., M. F. Baumgardner, R. A. Weismiller, L. L. Biehl, and B. F. Robinson. 1979. Extension of laboratory-measured soil spectra to field conditions. 1979 Machine Processing of Remotely Sensed Data Symp. Purdue University, West Lafayette, IN. pp. 253-262.

Stoner, E. R. and M. F. Baumgardner. 1980. Physiochemical, site, and bidirectional reflectance factor characteristics of uniformly moist soils. LARS Technical Report 111679. Laboratory for Applications of Remote Sensing, Purdue University, West Lafayette, IN.

United Nations Environment Program (UNEP). 1977. The State of the Environment: Selected Topics 1977. Decreasing agricultural base of food production: land and soil loss. Pergamon Press. New York. pp. 8-10.

Vanderbilt, V. C. 1981. Personal communication.

Weismiller, R. A. and S. A. Kaminsky. 1978. Application of remote sensing technology to soil survey research. J. Soil Water Conserv. 33(6):287-289.

Weismiller, R. A., I. D. Persinger and O. L. Montgomery. 1977. Soil inventory from digital analysis of satellite scanner and topographic data. Soil Sci. Soc. Am. J. 41(6):1166-1170.

Westin, F. C. and C. J. Frazee. 1976. Landsat data, its use in a soil survey program. Soil Sci. Soc. Am. J. 40(1):81-89.

Zachary, A. L., J. E. Cipra, R. I. Dideriksen, S. J. Kristof and M. F. Baumgardner. 1970. Application of multispectral remote sensing to soil survey research in Indiana. LARS Technical Report 110972. Laboratory for Applications of Remote Sensing, Purdue University, West Lafayette, IN.